Numerical Investigation of the Behavior of Pile Subjected to Uplift and Lateral forces

Firomsa Mekonnen Geleta

A Thesis Submitted to the Department of Civil Engineering

College of Civil Engineering and Architecture

Presented in Partial Fulfillment of the Requirement for the award of Degree of master's in civil engineering (Geotechnical Engineering).

November,2025

Adama, Ethiopia

Numerical Investigation of the behavior of pile subjected to uplift and lateral forces.

Firomsa Mekonnen Geleta

Advisor: Damtew Tsige (PhD)

A Thesis Submitted to the Department of Civil Engineering

College of Civil Engineering and Architecture

Office of Graduate Studies

Adama Science and Technology University

November,2025

Adama, Ethiopia

Declaration

I hereby declare that this MSc Thesis entitled “Numerical Investigation of the behavior of pile subjected to uplift and lateral forces” is my original work and has not been presented for a degree in any other University to any university for similar purpose. The references used in this thesis are duly recognized by proper citations.

Firomsa Mekonnen	_____	_____
Name of Student	Signature	Date

Recommendation of Advisors

I, the major advisor of this thesis, hereby certify that I have read the revised version of the thesis entitled "Numerical Investigation of the behavior of pile subjected to uplift and lateral forces" prepared under my guidance by Firomsa Mekonnen submitted in partial fulfillment of the requirement for the award of degree of Master of Science in Civil Engineering (Geotechnical Engineering).Therefore, I recommend the submission of the revised version of the thesis to the department following the applicable procedures.

Damtew Tsige (PhD)		
Major-Advisor	Signature	Date
Zerihun Lemesa (MSc)		
Co-advisor	Signature	Date

Approval Page of M.Sc. Thesis

I/we, the advisors of the thesis "Numerical Investigation of the behavior of pile subjected to uplift and lateral forces" developed by Firomsa Mekonnen, hereby certify that the recommendation and suggestions made by the board of examiners are appropriately incorporated into the final version of the thesis.

Damtew Tsige (PhD) _____ _____

Major-Advisor Signature Date

We, the undersigned, members of the Board of Examiners of the thesis by Firomsa Mekonnen have read and evaluated the thesis entitled "Numerical Investigation of the behavior of pile subjected to uplift and lateral forces" and examined the candidate during open defense. This is, therefore, to certify that the thesis is accepted for partial fulfillment of the requirement of the degree of Master of Science in Civil Engineering (Specialization in Geotechnical Engineering).

_____ _____ _____

Chairperson Signature Date

_____ _____

Internal -Examiner Signature Date

_____ _____ _____

External -Examiner Signature Date

Finally, approval and acceptance of the thesis are contingent upon submission of its final copy to the Office of Postgraduate Studies (OPGS) through the Department Graduate Council (DGC) and School Graduate Committee (SGC).

_____ _____

Department Head Signature Date

_____

School Dean Signature Date

_____ _____

Office of Postgraduate Studies, Dean Signature Date

Table of Contents

Lists of Figures

Lists of Tables

List of Symbols and Notations

	Boundary element method,
FEM	Finite Element Method
3D	Three Dimensional
2D	Two Dimensional
P-Y	Horizontal Load verses Deflection
L_C	Critical embedded pile length
LLP	laterally loaded piles
ULS	ultimate limit state method
Es	is the soil's modulus of elasticity
μ_s	Poisson's ratio of the soil
U	Lateral deflection of the pile at point z along the pile's length
Ep	Pile modulus of elasticity
k_h	horizontal coefficient of subgrade reaction
P	Soil pressure over the pile
D	Pile diameter
Ip	Pile cross section moment of Inertia
Q	Axial load on pile
SPTN	Standard Penetration Test Number
Gc	characteristic soil stiffness
Vult	Vertical Ultimate Capacity

Abstract

The increasing complexity of modern infrastructure, such as skyscrapers and transmission towers, means that deep foundations need to be designed in a new way. These buildings put a lot of stress on pile foundations because they have both lateral and uplift forces acting on them at the same time. Current design codes, like (API, 2011) and (DNV, 2021), usually examine at these loading parts separately. This makes things simpler, but it can also lead to designs that aren't safe or materials that aren't used efficiently. This study fills this important gap by using a complex three-dimensional finite element analysis to look at how single bored concrete piles interact with each other when they are loaded in both the uplift and lateral directions in stratified cohesive soils, which are similar to those found in the Addis Ababa Bole sub city. Using PLAXIS 3D CONNECT Edition V21, a thorough parametric study was carried out to simulate a realistic four-layer soil profile using the Mohr-Coulomb constitutive model. Using a range of loading scenarios, including pure uplift, pure lateral, and their combinations, the study methodically examined piles with different geometries (diameters: 0.6 m, 0.8 m, 1.0 m; lengths: 5 m, 10 m, 15 m). The accuracy of the numerical predictions has been verified by thoroughly validating the model against established field load test data. The findings clearly show that uplift and lateral loading mechanisms interact in a significant and negative way. Key findings show that concurrent uplift loads can increase lateral deflections at working loads by more than 25% and degrade lateral stiffness by up to 15%, while applying a lateral load equal to 75% of its pure capacity can decrease the uplift capacity by up to 12%. According to the study, shorter, stiffer piles have a more brittle failure mode and are disproportionately susceptible to these interaction effects. On the other hand, because of a deeper mobilization of soil resistance, longer, more flexible piles exhibit superior resilience. The development of useful, measurable design guidelines in the form of normalized interaction diagrams and capacity reduction factors is the main contribution of this study. With the use of these tools, practicing engineers can directly incorporate combined loading effects into pre-existing design frameworks. In order to improve pile foundations' safety, serviceability, and economic efficiency in quickly growing urban environments like Addis Ababa, this work firmly supports the incorporation of interaction analysis into standard geotechnical design practice.

Key Words: Single pile, Finite Element Plaxis 3D, Combined pull-out and lateral force

1. INTRODUCTION

1.1. Background of study

Pile foundations are predominantly employed to provide support for civil engineering structures, including bridges and multi-story buildings, particularly in scenarios where the upper soil strata exhibit significant compressibility and lack the required strength to bear the loads transferred from the superstructure. This foundation is particularly pertinent when the bedrock is not located at a sufficiently shallow depth beneath the surface of the ground, and when the structures are subjected to horizontal forces as well as the need to counteract bending moments and vertical loads. These piles are specifically designed to accommodate vertical loads, lateral loads, or a combination however, due to the intricacies involved in the analysis of piles under combined loading conditions, contemporary practices typically involve an independent analysis of piles with respect to vertical loads to ascertain their deformation and settlement characteristics, as well as an analysis for lateral loads to evaluate their flexural behavior (Karthigeyan et al., 2007). This chapter provides a thorough examination of the numerical investigation findings pertaining to single piles subjected to combined uplift and lateral loading within layered cohesive soil contexts. The discourse centers on quantifying interaction effects, scrutinizing layer-specific responses, and formulating pragmatic design recommendations. All findings were derived utilizing PLAXIS 3D, with the Mohr-Coulomb model parameters delineated in Chapter 3

The investigation of the interaction of uplift loads on the lateral capacity of piles subjected to combined loads reveals a deficiency in systematic analysis, and the extant literature in this domain remains notably limited. There is some information available on this topic that comes from field research, analytical studies, and experimental investigations.

Piles are fundamentally employed to endure vertical compression, uplift, and horizontal or inclined forces (Spagnoli G. and Tsuha C. de Hollanda Cavalcanti, 2020) and (Malhotra H. and Singh S. K., 2022). They serve a crucial role in counteracting uplift forces in bridge foundations, abutments, and tall structures that are vulnerable to overturning loads induced by environmental factors such as wind and waves.

Furthermore, piles possess the capability to mitigate settlement (P, 2020) by situating their tips above soil strata characterized by high compressibility. The self-weight of the pile, in conjunction with the skin friction acting along its surface, contributes to the resistance against uplift forces (Reddy K. Madhusudan and Ayothiraman R., 2015). In recent times, there has been a marked increase in the construction of transmission towers, high-rise edifices, and other tall structures. The foundational system must also possess the capacity to counteract vertical uplift forces to align with the design specifications of these engineering constructs (Kranthikumar A., Sawant V. A., and Shukla S. K., 2016). For numerous years, geotechnical engineering has employed piles or pile foundations to transfer and support loads onto soils deemed to possess inadequate structural integrity due to their prevailing conditions

Furthermore, an augmentation in the embedment ratio and the relative density of sand culminates in an elevated ultimate pullout capacity (Fakher N. and Fakhruldin M.,, 2021). The assessment of soil deformation in the vicinity of the pile is imperative for the reliable design of structures to withstand pullout forces, as articulated by Faizi et al. (2015). They substantiated the results from laboratory tests through the application of finite element method software, elucidating that soil deformation is intrinsically related to density and is contingent upon its dilatancy characteristics. Lozovyi et al. (2014) employed a finite element program to execute four static pile tests, facilitating the calculation of pile settlements. The findings were subsequently juxtaposed with full-scale pile tests to ascertain the influence of reaction piles on the response of the tested pile. To facilitate this investigation, simulations were executed incorporating a cluster of reaction piles encircling the tested pile, applying the corresponding negative loads. A robust correlation was identified between the load-displacement curves derived from in situ measurements and those procured via Plaxis. Moreover, recommendations were proffered for the enhancement of Plaxis modeling techniques. This study utilizes a finite element model within Plaxis 3D (Alasadi A. A. and Mustafa F. S., 2022) to replicate the behavior of an individual pile within sandy soil subjected to pullout force, employing experimental data for validation derived from a real-world case study.

In light of this, my research paper concentrates on the examination of piles subjected to a combination of vertical and lateral loads through the implementation of 3D finite-element analyses. The intricacies of the numerical model, the validation of the developed model against several field test cases, as well as the outcomes from parametric studies will be elaborated upon in the paper.

1.2. Statement of the Problem

The global transition towards taller and more slender edifices has imposed distinct requirements on deep foundation systems. Pile foundations intended for such infrastructural developments are progressively subjected to complex; multi-directional loading conditions wherein uplift and lateral forces coexist simultaneously. Nevertheless, the prevailing state of practice, frequently informed by standards such as (API, 2011), predominantly relies on methodologies that regard axial and lateral responses as isolated phenomena. This disjointed analytical framework is increasingly acknowledged as insufficient, potentially culminating in:

1. Non-conservative Designs: A tendency to underestimate pile head deflections and overestimate ultimate capacity, thereby jeopardizing structural integrity.

2. Inefficient Designs: An inclination towards overly conservative pile dimensions due to the inability to accurately assess the genuine capacity of the system, resulting in superfluous material and financial expenditures.

In the particular context of Addis Ababa's rapid construction boom, this challenge is particularly pronounced. The construction of high-rise structures in the Bole district necessitates pile foundations capable of effectively resisting substantial uplift forces induced by overturning moments from wind and seismic activities, concurrently with lateral loads stemming from earth pressure and structural dynamics. Preliminary numerical investigations (e.g., Witasse, 2025) indicate that neglecting the interaction between these loads may result in a reduction of lateral capacity by as much as 20%. Regionally, investigations conducted by (Mungure, 2016) and (Nakabuye et al., 2019) have underscored a pervasive deficiency of site-specific research that addresses nonlinear soil-pile interactions within African geotechnical contexts.

A significant lacuna exists at the local level: there is a total absence of systematic, quantitative investigations scrutinizing the impact of combined uplift and lateral loading on pile foundations within the stratified cohesive soils of Addis Ababa, specifically in the Bole area. This knowledge deficit hinders the optimization of foundation design, potentially leading to either safety hazards or economically inefficient solutions. Therefore, this study endeavor is structured to address this gap by employing advanced numerical modeling techniques to provide a comprehensive analysis of this interaction, yielding practical insights that are attuned to local conditions.

1.3. Research Questions

The study will address the issues raised through investigation of the following research questions:

1. In what way do simultaneous uplift forces affect the lateral load-deflection behavior, and ultimate capacity of single piles installed in stratified cohesive soils?
2. What are the specific mechanisms of soil-pile interactions at layer interfaces, and in what ways do they affect the overall system behavior when subjected to combined loading conditions?
3. How do pile embedment depth and pile diameter change the uplift-lateral interaction effects?

1.4. Objective

1.4.1. General Objective

The general objective of this research is numerical investigation of the behavior of pile subjected to uplift and lateral forces in layered soils using Plaxis 3D finite element software.

1.4.2. Specific Objective

The specific objectives of this research work are:

- To investigate the effects of uplift force on lateral load capacity pile foundation
- To investigate the critical load combination ratio (Uplift Force / Lateral Force) that leads to the most significant reduction in overall performance.
- To investigate the effects of pile length and diameter on combined loaded single pile.

1.5. Significance of The Study

The outcomes of this investigation possess considerable importance for both engineering applications and scholarly knowledge:

For Ethiopian Infrastructure Development: This research furnishes essential, context-specific data along with design protocols for the secure and cost-effective design of pile foundations within the layered cohesive soils of Addis Ababa. Such contributions are directly relevant to the design of high-rise structures, bridge abutments, and other pivotal infrastructure, thereby enhancing the

safety and sustainability of the nation's ongoing urban development.

Advancement of Design Practice: Through the formulation of pragmatic interaction diagrams and the quantification of capacity reductions, this study provides engineers with a concrete methodology to advance beyond simple, decoupled design strategies. This progression results in more dependable foundations that neither fall into the pitfalls of severe under-design nor the excesses of unnecessary over-design, thereby optimizing the utilization of materials and costs.

Contribution to Geotechnical Knowledge: This research enriches the global compendium of knowledge surrounding soil-structure interaction under multifaceted loading conditions, especially concerning layered soil profiles that are frequently oversimplified in existing scholarly discourse. The validated PLAXIS 3D model functions as a reference point for forthcoming investigations within similar geotechnical contexts.

Reduction of Reliance on Costly Field Testing: The investigation illustrates the effectiveness of advanced numerical modeling as a viable instrument for thorough parametric analysis. This advancement may diminish the reliance on extensive and financially burdensome field load-testing regimes, thereby permitting the exploration of a broader array of scenarios in a virtual environment at a significantly reduced cost.

1.6. Limitation and Scope of the Study

This research focuses specifically on the following scope:

1. Soil Conditions: The study is limited to cohesive soils (clays) with layered profiles, excluding granular materials and mixed soil conditions.
2. Pile Type: Analysis is conducted for single, vertical, bored concrete piles with circular cross-sections, without considering pile groups or inclined piles.
3. Loading Conditions: The research considers static loading conditions only, excluding dynamic, cyclic, or seismic loading scenarios.
4. Modeling Approach: The study employs the Mohr-Coulomb constitutive model with effective stress parameters, acknowledging that more advanced models could provide additional insights.

The main limitations of the study include:

- ❖ The use of "wish-in-place" pile installation rather than modeling actual installation effects.
- ❖ The assumption of linear elastic pile material behavior.
- ❖ The focus on a specific range of soil parameters and layer configurations.

1.7. Organization of the Thesis

There are six chapters in the thesis. Details about the work's title and primary goal are covered in the first chapter. The second chapter will provide a review of the literature. Research approach is labeled in Chapter 3. The various parameters and the results of the validation study of numerical modeling are described in the fourth chapter. The parametric study's findings and discussion are presented in Chapter 5. Additionally, chapter six provides a general conclusion, a summary of the work done in the preceding chapters, and suggestions for potential future research.

2. Literature Review

2.1. Introduction

The design of pile foundations of modern structures such as offshore wind turbines, power pylons, and bridge piers ever more requires information on their response under advanced combined loading conditions. Such structures are likely to transfer high lateral loads of environmental loads (wind, waves, currents) along with tensile/uplift forces of overturning moments or working tensions on their foundations. Codes of historical design, e.g., the American Petroleum Institute (API, 2011) and Det Norske Veritas (DNV, 2021), generally consider lateral and axial responses individually, which can lead to non-conservative designs or an overestimation of the system stiffness (Byrne et al., 2020). This chapter provides a critical review of the literature on the lateral and uplift response of single piles, specifically recent advances in understanding how they respond under combined loading. It also accounts for the evolution of numerical modeling techniques, particularly 3D Finite Element Analysis (FEA) with advanced constitutive models, to bridge the gap between simplified design methods and real-world complexity.

2.2. Lateral Response of Single Piles: From p-y Curves to Advanced Modeling

The analysis of laterally loaded piles remains dominated by the p-y curve method, an empirically based approach that models the soil as a series of non-linear springs.

The p-y curve method relates the nonlinear behavior between the soil resistance *(p)* and the lateral pile deflection *(y)*. The plot of the p and y variables at depth is called the p-y curve, (Haiderali and Madabhushi, 2016). The *p-y* curves are derived and validated by performing field tests on fully instrumented piles. In 1950s, the full-scale testing for laterally loaded piles was possible because of two main developments at that time: (a) the availability of digital computers to solve Eq. 2.2 and, (b) the ability for remotely reading the strain gauges to obtain the soil response, (Lymon C.Reese and William F.Van Impe, 2011). The method implicitly accounted for the soil continuity and the nonlinearity of the pile-soil system; however, its main shortcoming is that the p-y curve is unique for a particular soil and pile properties, (Horvath and Colasanti, 2011). Owing to the popularity of the p-y curve method and its reasonable results, it was suggested to be used in engineering practice by (API, 1987 and 2007). Furthermore, (FHWA, 2011) recommended the use of LPILE or FBPIER software that use the p-y curve method, in the analysis of laterally loaded piles, (Favaretti et al.,

2015).

2.2.1. Standard P-y Procedures and Limitations

API (2011) industry-standard procedures for soft clay as suggested by Matlock (1970) and stiff clay as suggested by Reese et al. (1975) are widely used. The procedures correlate the soil resistance (p) with pile deflection (y) using the undrained shear strength (s_u) and a reference strain parameter (ε_{50}). Nonetheless, a significant limitation lies in their calibration for laterally loaded piles without consideration of stress path dependencies and the influence of simultaneous axial loading (Li, Liu, & Wu, 2022). Further, the empiricism involved in p-y curves makes their reliability highly site-specific.

2.2.2. Recent Refinements and Critiques

Recent research has focused on p-y curve refinements.

As an example, Becker et al. (2018) utilized centrifuge test results of monopiles in clay to show that traditional API curves would be too conservative for large diameter monopiles, as they cannot analyze the 3D failure wedge and soil flow mechanisms accurately. Similarly, Yu et al. (2021) proposed a p-y curve correction for soft clay considering the influence of cyclic loading in an improved manner, showing how stiffness loss under cycles can significantly contribute to long-term response. These works indicate the growing view that standard p-y methods require context-dependent adjustments, especially for novel foundation types and loading scenarios. 2.3. Uplift Capacity and Tensile Load-Deformation Behavior

Shaft adhesion is the predominant controlling parameter for the uplift capacity of piles in clay and relies on undrained shear strength and pile-soil interface properties (Kulhawy, 1985). Short-term capacity can be improved by suction effects under undrained conditions, though this generally is neglected in design due to its transient nature.

Recent Research: Sheil and McCabe (2020) investigated the tensile load-transfer of piles in glacial till using field tests and numerical modelling.

They emphasized the importance of possessing a good model of the load-deformation response over the ultimate capacity, as serviceability conditions generally govern design. They proved that mobilization of shaft resistance is non-linear and is dependent on pile roughness and soil stress history. This focus on the complete load-deformation curve, rather than the simple single capacity value, is crucial for understanding the interaction between uplift forces and lateral loads before

ultimate failure.

2.4. Piles under combined lateral and uplift loading: The Interaction Effect

The principal theme of this thesis is with the interaction between these two modes of load. Independent superposition of capacities is increasingly regarded as inadequate.

2.4.1. Experimental Evidence

Early field testing by Ismael (2001) and centrifuge tests by Peng et al. (2011) gave clear-cut evidence that tensile loads degrade lateral performance. Recent experiments have quantified and verified these results. Liu et al. (2020) had also conducted a series of centrifuge tests on model piles installed in soft clay under combined loading. Their results had indicated that application of a tensile load would increase head lateral deflection by over 50% at an imposed lateral load and significantly increase the maximum bending moment. They assigned this to a reduction in the effective confining stress around the pile, lowering the passive resistance of the soil.

2.4.2. Numerical Studies and Parametric Developments

The Finite Element Method has emerged as the primary technique for studying this interaction in depth due to the cost and complexity of physical modeling.

- **Early Numerical Studies:** Authors like Karthigeyan et al. (2007) and Lin et al. (2014) laid the groundwork, with their conclusion being that loss of lateral capacity due to tension is larger for softer grounds and for shorter piles.
- **Current High-Fidelity Simulations**: Recent studies benefit from more sophisticated computer software. Liu & Wang (2019) performed a 3D FEA using an advanced constitutive model and successfully showed that the occurrence of tensile load not only reduces the ultimate lateral capacity but also alters the depth and shape of the bending moment, shifting the maximum point moment towards the mudline. Liu, Z. et al. (2023) conducted a comprehensive numerical parametric analysis of offshore monopiles with direct consideration of tension's effect on dynamic lateral response. The pile-soil system natural frequency is seen to reduce as the tensile load intensifies, something of great concern for dynamically sensitive structures like wind turbines.
- **Suggested Design Modifications:** One of the key elements of ongoing research is the transition to design modifications. Liu et al. (2020), from the data of their centrifuge, proposed

an interaction relationship reducing the modulus of the p-y curve (E_{py}) as a function of the tensile applied load ratio (T/Tult). Similarly, Liu & Wang (2019) presented a reduction factor for the ultimate soil lateral resistance (pult) under tension conditions.

2.3. Numerical Modeling Enhanced with PLAXIS 3D

PLAXIS 3D is best practice geotechnical FEA due to its robust treatment of soil-structure interaction.

2.3.1. Constitutive Model Development

Evolution from simplification to sophisticated models is today's best practice. The Hardening Soil (HS) model, where stress-dependent stiffness and multiple stiffnesses for initial loading and unloading/reloading are considered, is a significant improvement (Brinkgreve et al., 2020). The Hardening Soil with Small-Strain Stiffness (HSSmall) model is particularly well-adapted to this problem because it incorporates the very high initial stiffness of soil at small strains (Benz, 2007), which governs serviceability limit states at working loads. Tsiampousi et al. (2021) demonstrated the importance of employing the HSSmall model in the description of deep excavation deformation, a problem with similar stress-path complexities as laterally loaded piles.

2.3.2. Modeling and Interfaces for Pile Installation

One major advancement is the shift toward simulating installation. While "wish-in-place" remains common, studies more and more simulate installation effects by creating a "smear zone" of remolded soil adjacent to the pile with reduced strength and stiffness parameters (Brinkgreve et al., 2020). Interface element calibration (with R_inter) is also essential for simulating slip and gap development, fundamental mechanisms under combined uplift and lateral loading (Plaxis, 2022).

2.4. Research Gaps Identified and Contribution of This Study

Even with recent advances aside, certain gaps warrant the current study:

- Systematic Parametric Study in Layered Soil: Although there are a number of numerical investigations, there is still a need for a detailed parametric study utilizing the Mohr-Coulomb model in PLAXIS 3D, focusing on layered cohesive soils under changing strength profiles and sequences of layers.
- Direct Modification of API p-y Curves for Layers: The majority of studies provide capacity reduction interaction equations. There are few that provide direct, engineering-perspective

modifications to the design formulation of the reference API p-y curves for clay to incorporate uplift forces in layers. This would be a simpler contribution to the daily design practice.

- ❖ Focus on Serviceability Stiffness of Layered Systems: Literature predominantly focuses on ultimate capacity. Degradation of initial lateral stiffness (a most important serviceability parameter) due to uplift force requires quantification on a wider range of pile geometries and layered soils. Dave Exploration.

This research will complete these gaps by conducting extensive numerical analysis in PLAXIS 3D using the Mohr-Coulomb model for multi-layered soil. The outcome will be a clear set of guidelines and correction factors to update typical lateral pile analysis for the detrimental effect of combined uplift forces in real multi-layered soil deposits.

2.5. Ultimate Lateral Resistance

Lateral pressures and movements for structures on pile foundations can be caused by significant wind forces in transmission-tower foundations, retaining walls, ship impact and wave action in harbor and offshore buildings, and lateral accelerations operating on structures in seismic zones. Therefore, figuring out the ultimate lateral resistance could be a major pile design difficulty. (B.Hansen, 1961), (B.B. Broms, 1964a, b, 1965), and other methods have been proposed to find the ultimate lateral load capacity Hu. Broms' method is one of the most popular methods for estimating Hu, according to Lee et al. (2010). Three times the passive Rankine earth pressure is thought to be the ultimate soil resistance for unrestrained or free-headed piles (B.B. Broms, 1964a, b, 1965) (H.G. Poulos and E.H. Davis, 1980).

A pile was subjected to a horizontal load test, which involved positioning two piles at a certain distance apart and either pushing or pulling them toward one another. For a single pile, the resultant load displacement curve plots the horizontal load Ho against the horizontal displacement yo (Figure 2.4). According to this curve, the horizontal load Ho that corresponds to a displacement equal to a tenth of the pile diameter (B/10) is the ultimate load (Briaud, 2013).

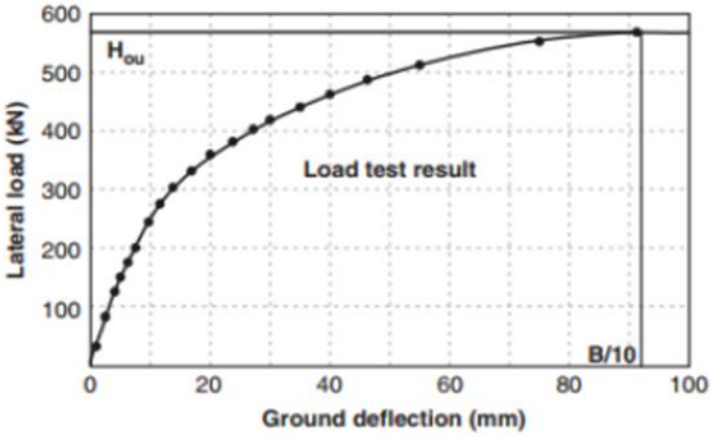

Figure 2.1: Load test result *(Briaud, 2013)*

Furthermore, the yield of the maximum permitted lateral displacement at the pile head—which is assumed to be 10% of the pile diameter because it is more in line with the design criterion—is the control factor in determining the ultimate lateral load capacity of the piles in the finite element method (ASTM STP-835, 1983 and USACE, 1998).

When it is challenging to determine the ultimate limit state from the loading deflection curve, the ultimate horizontal load measured at deflection equals 10% of the pile's diameter, as per British Standard as advised in BS EN 1997-1:2004+A1:2013, 7.6.1.1(3).

2.6. Constitutive Models

Soil is a complex material that behaves non-linearly under stress, often displaying anisotropic and time-dependent behavior. When it comes to main loading, unloading, and reloading, soil usually displays unique tendencies. It exhibits non-linear behavior well below the failure condition with stress-dependent stiffness. Soil exhibits minor strain stiffness, plastic deformation, and irregular dilatancy at very low strains and during stress reversal. Its failure in a three-dimensional condition of stress is quite complex, aside from the behavior of the soil. To explain why a material might fail in such a stress situation, numerous criteria have been established.

Using a suitable constitutive model for a given geotechnical problem in finite element analysis can result in accurate predictions. Generally speaking, the evaluation criteria for soil models should always strike a balance between the demands of laboratory testing for realistic representation of soil behavior, the requirements of continuum mechanics, the ease of deriving parameters, and the ease of

computational application. A brief discussion of the employment of some constitutive models in the Plaxis finite element model for this investigation is given below.

2.6.1. Linear Elastic Model

The linear elastic model is commonly used to represent large structures, such piles, that are located in soil or bedrock layers (R.B.J. Brinkgreve and W. Broere, 2006). Hooke's equation of isotropic linear elasticity is used to model the pile material's stress-strain relationship. The linear elastic constitutive model is probably the most widely used model for estimating the stress-strain relationship of materials. In linear elastic models, the two elastic stiffness parameters that are utilized are Young's modulus (E) and Poisson's ratio (v). Because soil is highly nonlinear and irreversible, the linear elastic model is ineffective for simulating it. However, it is good for simulating stiff volumes in soil, like concrete structures.

2.6.2 Mohr Coulomb Model

A linearly elastic and completely plastic model is the Mohr Coulomb model. Five factors are involved: the dilatancy angle (ψ), the friction angle (ϕ) and cohesion (c) for soil plasticity, the Young's modulus (E) and Poisson's ratio (v) for soil elasticity.

Hook's law assumes that the stiffness behavior below the failure line is linearly elastic. As a result, the model is unable to anticipate deformation prior to failure, particularly when stress levels are fluctuating or numerous stress routes are permitted. After peak strength, the model does not exhibit softening behavior, though. Mohr-Coulomb's model would predict a constant mean effective stress in this situation, which leads to an overestimation of the shear strength. In contrast, soft soils, such as typically consolidated clays, typically exhibit a decreasing mean effective stress during undrained shearing (Plaxis 3D Foundation Manual, 2006).

The soil in the problems of this paper is modeled as elastic-plastic material. The basic principle of elasto-plasticity is that strains and strain rates are decomposed into an elastic part and plastic part as shown in Figure 2.2.

Stress rates and elastic strain rates are related using Hooke's law. Plastic strain rates are proportional to the derivative of the yield function with respect to stresses, as per the classical theory of plasticity. Thus, it is possible to depict the plastic strain rates as vectors that are perpendicular to the yield surface.

The term "associated plasticity" refers to this traditional version of the idea. The hypothesis of linked plasticity, however, overestimates dilatancy for Mohr-Coulomb type yield functions (Plaxis 3D Foundation Manual, 2006).

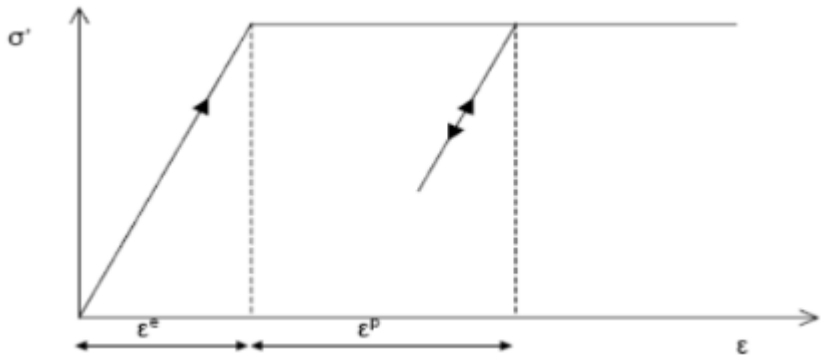

Figure 2.2: Basic idea of an elastic perfectly plastic model *(R.B.J. Brinkgreve and W. Broere, 2006)*

Coulomb's friction law is extended to general stress conditions by the Mohr-Coulomb yield condition. Actually, on any plane within a material element, this condition guarantees that Coulomb's friction law is obeyed. When expressed in terms of primary stresses and six plastic potential functions, the complete Mohr-Coulomb yield is composed of six yield functions (Plaxis 3D Foundation Manual, 2006).

Both the cohesiveness c and the well-known friction angle ϕ are plastic model factors that show up in the yield functions. A third plasticity parameter, the dilatancy angle ψ, is present in the plastic potential functions. Dilatancy, or positive plastic volumetric strain increments, as they are observed in dense soils, must be modeled using this parameter. As previously mentioned, the behavior is elastic and follows Hooke's rule isotropic linear elasticity for stress states within the yield surface (Plaxis 3D Foundation Manual, 2006).

2.7. Conclusion

Literature conclusively indicates that independent analysis of lateral and uplift pile behavior separately is not sufficient for modern engineering practice. Experimental and advanced numerical studies last decade consistently validated that tensile actions significantly underrate the stiffness and capacity of laterally loaded piles by reducing soil confinement and modifying failure mechanisms. The availability of sophisticated FEA software like PLAXIS 3D presents a distinct opportunity to measure in a controlled manner these interactions in stratified soils and transform the findings into useful

engineering design recommendations. This thesis will expand on this foundation to provide actionable conclusions for the pile design under combined loading in stratified ground.

3. Methodology of Study

3.1. General description of study area

3.1.1. Site Location and Project Context

The geotechnical parameters anchoring this numerical study were sourced from a comprehensive site investigation report for a proposed 2B+G+10 Mixed-Use building in Addis Ababa, Bole sub city around Millennium. This specific location is emblematic of the city's rapid vertical development, where high-rise structures with deep basements are becoming commonplace. The selection of this site ensures the research is grounded in a realistic and relevant geotechnical context, addressing the actual challenges faced by practicing engineers in the region.

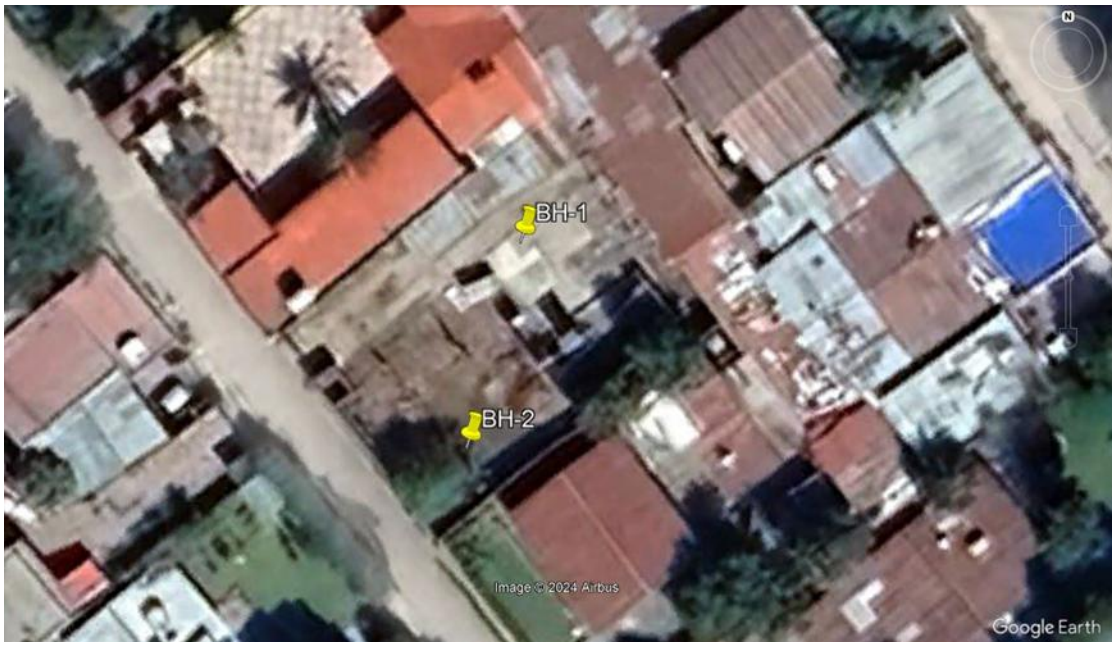

Figure 3.1: Satellite image of the project area with borehole locations

3.1.2. Site Geology and Subsurface Characterization

The uppermost layer of the project site is Backfill material silt, clay and gravel soil, which extends up to a depth of 0.30m in both BH-1 and BH-2. Beneath the upper layer of the project site is characterized as Medium stiff to stiff, dark grey, Fat CLAY soil layer, which extends up a depth of 2.80m and 3.00m around BH-1 and BH-2 respectively. Beneath layer B is Stiff to very stiff, light grey, Elastic SILT/ Fat CLAY/ Silty GRAVEL layer, which extends up to a depth of 13.00m and 11.00m around BH-1

and BH-2 respectively. Beneath layer C is Stiff to very stiff, light grey to brown, Elastic SILT with sand/ Sandy SILT soil layer, which extends up to a depth of 15.00m and 13.00m around BH-1 and BH-2 respectively. Beneath layer D is Stiff to very stiff, light grey to brown, Elastic SILT with sand/ Sandy SILT/ SILT with sand soil layer, which extends up to a depth of 18.00m and 15.00m around BH-1 and BH-2 respectively. The lowest profile of the project site is Very stiff to hard, light grey to dull white, Lean CLAY with sand/ Silty GRAVEL with sand/ SILT/ Sandy Fat CLAY soil layer, which extends up to ends of exploration depth in both boreholes.

Geotechnical Cross Section through BH-1 and BH-2

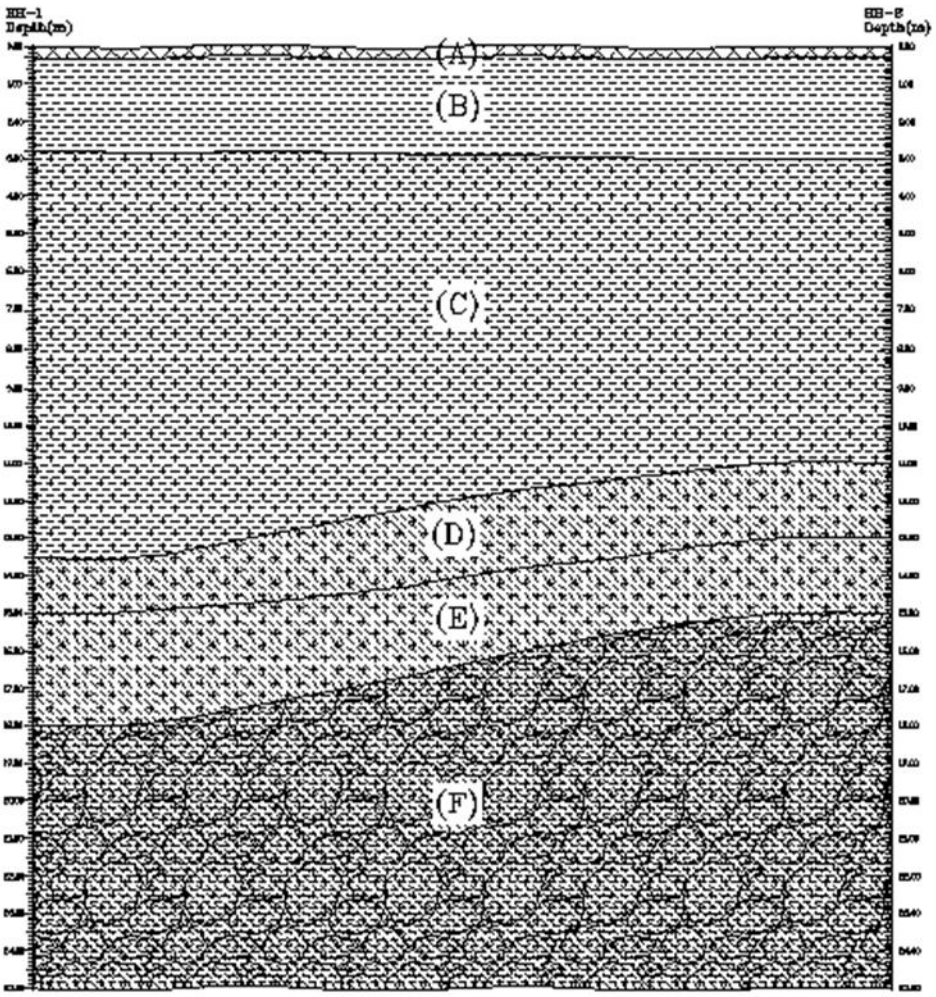

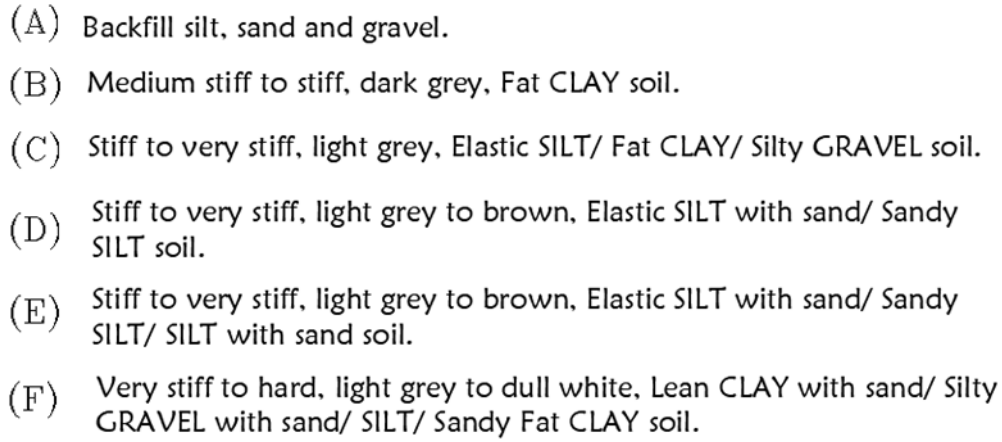

Figure 3.2: Selected geological profiles

The generalized soil strata are as follows:

- **Layer 1 (0 - 4m):** Backfill and Fat CLAY. This upper stratum consists of recently placed fill material underlain by a layer of medium stiff to stiff, dark grey, fat clay. This layer has low permeability and is susceptible to volume changes with varying moisture content.
- **Layer 2 (4 - 12m):** Elastic SILT/Fat CLAY. This thick intermediate layer is characterized as stiff to very stiff, light grey, elastic silt interbedded with lenses of fat clay. The "elastic" nature suggests a significant recoverable deformation component, which can influence the pile's response under cyclic loading.
- **Layer 3 (12 - 16m):** Sandy SILT/Elastic SILT with sand. A transitional layer of stiff to very stiff, light brown, sandy silt. The increased sand content suggests a higher permeability and friction angle compared to the overlying layers.
- **Layer 4 (16m+):** Lean CLAY with sand/Silty GRAVEL. The deepest layer encountered is very stiff to hard, comprising a variable mix of lean clay, silt, and gravelly sand. This layer provides a competent bearing stratum for end-bearing piles.

A critical finding was the absence of groundwater within the depth investigated. This allows for a drained analysis to be representative for long-term conditions, simplifying the initial modeling phase, though undrained scenarios could be explored in future work for short-term or sudden loading events.

3.2. Research Methodologies and Theoretical Approach

This research adopts a quantitative, simulation-based methodology rooted in the model of numerical experimentation. Given the prohibitive cost and time associated with full-scale testing of piles under combined loading, the Finite Element Method (FEM) provides a controlled, repeatable, and detailed alternative to investigate this complex soil-structure interaction problem. The overarching workflow, illustrated in Figure 3.3 below, was designed to ensure a systematic and validated investigation.

Figure 3.3: Research Methodology Workflow

1. **Problem Definition & Literature Review:** Identify knowledge gaps and define scope.
2. **Site Data Synthesis:** Collate and interpret geotechnical reports to develop representative soil models.
3. **Numerical Model Development:** Create 3D FEM geometry, assign materials, and define boundaries.

4. **Model Calibration & Validation:** Adjust model parameters to match a known field case, ensuring predictive reliability.
5. **Parametric Study Execution:** Run the predefined matrix of analyses in PLAXIS 3D.
6. **Results Extraction & Processing:** Collect data on forces, displacements, and stresses.
7. **Data Analysis & Synthesis:** Interpret results to identify trends, quantify interactions, and develop design aids.
8. **Conclusion & Recommendation:** Draw final conclusions and propose practical design guidelines.

3.3. Derivation of Model Parameters

3.3.1. Soil Parameters: From Field Data to Constitutive Model

The Mohr-Coulomb (MC) elastoplastic model was selected to represent the soil strata. While advanced models like the Hardening Soil model offer more refined simulations of soil stiffness, the MC model was deemed appropriate for this study due to its simplicity, well-established use in practice, and the primary focus on ultimate limit state capacity under combined loads. Its parameters are also more readily derived from standard site investigation data.

Identifying parameters for the base model from in-situ tests or correlations of parameters are the fundamental components for analyzing piles subjected to uplift and lateral stresses. In light of the geotechnical investigation conducted by Arcon Design-built Plc (2024), a representative value of SPT test data is picked, and the necessary correlations between soil parameters are employed and chosen according to the quality, consistency, availability, and profile of the data. PLAXIS 3D uses soil parameters that are derived from the correlation between laboratory tests and SPTN results as input parameters. In table 3.1, these parameters are displayed.

A detailed explanation of the derivations is provided below:

Unit Weight (γ): Estimated based on soil description and typical values for cohesive soils.

Effective Cohesion (c') and Friction Angle (φ'): Correlated from SPT N-values using empirical relationships specific to clayey and silty soils. The increasing trend with depth reflects the over-consolidation ratio and the transition to denser, more competent materials.

Young's Modulus (E'): This is a critical parameter. For cohesive soils, E' was estimated as a multiple of the undrained shear strength (s_u), which itself was correlated from SPT N-values. The values were cross-checked with correlations of the form $E' = 200cu(1 + v)$.

Poisson's Ratio (ν'): A value of 0.3 was assumed for drained analysis, representative of the elastic behavior of saturated clays under fully drained conditions.

Dilatancy Angle (ψ): Set to 0° for normally to lightly over-consolidated cohesive soils, as they typically exhibit compressive rather than dilative behavior during shear.

Interface Reduction Factor (R_inter): This parameter is vital for modeling the soil-pile interaction. A value of 1.0 represents a perfectly rough interface, while 0.0 represents a perfectly smooth one. The values chosen (0.7 to 0.9) reflect the typical range for concrete piles in clay, increasing with soil stiffness, as a stiffer soil can mobilize more interface resistance.

Table 3.1: Mohr-Coulomb Parameters for Layered Soil Profile

Parameter	Symbol	Layer1 (0-4m)	Layer2 (4-12m)	Layer3 (12-16m)	Layer4 (16-40m)	Unit
Thickness	-	4	8	10	24	m
Unit Weight	γ	17	17.5	18	18.5	kN/m³
Effective Cohesion	c'	12.96	14.11	16	18.38	kPa
Effective Friction Angle	φ'	24°	26°	30°	29°	Degrees (°)
Young's Modulus	E'	4,500	4,800	5,400	6,000	kPa
Poisson's Ratio	ν'	0.3	0.3	0.3	0.3	-
Dilatancy Angle	ψ	0°	0°	0°	0°	°
Interface Factor	Rinter	0.70	0.8	0.85	0.9	-

3.3.2. Pile Parameters and Structural Modeling

To understand how pile characteristics impact the lateral response of individual piles, a variety of piles are included. The next sections discuss the parameters and their practical applications.

The bored concrete piles were modeled as linear elastic, non-porous volume elements. The assumption of linear elasticity is reasonable for reinforced concrete under serviceability limit states, which is a primary focus of this study. The parameters, detailed in Table 3.2, are standard for C30 grade concrete

The research considered the piles' three lengths and four diameters. Table 3.2 lists the parameters for the linear elastic model that was used to model the piles.

Table 3.2: Pile parameters used in the numerical analysis

Material	Symbol	Concrete	Concrete	Concrete	unit
Material model		Linear elastic	Linear elastic	Linear elastic	
Drainage type		Non-porous	Nonporous	Nonporous	
Modulus of elasticity	E	31	31	31	GPa
Poisson's ratio	v	0.15	0.15	0.15	-
Unit weight	γ	25	25	25	k/m^3
Length	L	5	10	15	m
Diameter	D	0.6	0.8	1.0	m

3.4. Comprehensive Parametric Study Matrix

To ensure a thorough exploration of the problem, a full-factorial parametric study was designed. This approach allows for the isolation of the effect of each variable and the investigation of potential interactions between them. The matrix, detailed in Table 3.3, was designed to be exhaustive, resulting in 84 unique numerical experiments

The parametric study investigates the interaction effects in layered soil conditions:

Table 3.3: Parametric Study Matrix

Case Group	Variable	Levels	Constant Parameters	Total Cases
Geometry	Length x Diameter	3 x 4 = 12 combinations	T/Tult=50%, Free head	12
Loading	Uplift Ratio (T/Tult)	0%, 25%, 50%, 75%		48
Analysis Type	Drainage Condition	Drained, Undrained A	24	24
Total Analysis Cases			84	84

And, the parametric study will focus on large-diameter bored piles, construction:

- Pile Length (L): 5 m, 10m, 15 m (to investigate embedment into the competent rock layer).
- Pile Diameter (D): 0.6 m, 0.8 m, 1.0m. This creates a 3x3 matrix for a total of 9 primary pile geometries.

4. Numerical Modeling

4.1. Introduction

The influence of uplift force on the lateral response of piles in the soils of the research region was examined in this study using numerical modeling. The accuracy of the numerical model results was controlled by verifying the study using full-scale load test results from the literature. A parametric investigation has been carried out following the verification of the finite element analysis solution (chapter 5). Variations in variables including the pile's diameter, uplift loads, and embedment depth will be examined. All analyses were conducted using Plaxis 3D V21 connect edition, a three-dimensional geotechnical finite element program. For a better understanding of the model designs, the properties and primary purposes of the 3D finite element methods were briefly introduced in this chapter.

4.2. Use of PLAXIS 3D CE V21 as Numerical modeling tool

An intuitive user interface and comprehensive 3D modeling capabilities are combined in PLAXIS 3D CE v21, a comprehensive three-dimensional finite element program. In 2010, the initial PLAXIS 3D software was made available. In geotechnical engineering and design, it is designed to analyze groundwater flow, stability, and deformation. There are five steps in the PLAXIS 3D CE v21 modeling method. Water levels, soil stratigraphy, structural components, discretization and transformation of the model geometry into finite elements, and calculation settings and calculations for soil, structures, mesh, flow conditions, and staged construction are all done using these mode tabs in PLAXIS 3D. In terms of constitutive models, PLAXIS 3D CE v21 includes a user-defined option along with a variety of diverse material models. These include the Mohr-Coulomb model (MC), the Hardening Soil model (HS), the Modified Cam-Clay model (MCC), the Linear Elastic model (LE), and alternatives. Plaxis 3D (2021).

Plaxis 3D provides thorough methods for documenting the analysis's conclusions. All of the numerical analysis's findings were shown by the output software in a variety of formats, including tables, graphs, and curves. The impacts of stresses and deformations make up the majority of it. Additionally, force results for structural components are displayed. This chapter introduces the specifics of the finite element modeling, material properties, and constitutive models used in the finished parametric study.

4.2.1. PLAXIS volume pile

The volume pile is composed of interface pieces that simulate the interaction with the surrounding dirt and volume elements. The volume pile in PLAXIS 3D can be built in two ways. Using the "Insert Solid" function, the first one involves determining the volume element's shape and location (see Figure 4.1). The second involves using the "command box," which defines the volume pile by virtue of its length, radius, and number of pile shaft segments.

The properties of the volume pile are properties. For example, to assign the volume pile which has properties of the $unit\ weight\ \gamma = 25\ kN/m^3$ and the Young's modulus $E = 3.10^7\ kN/m^2$, "soil and interface" material type and "linear elastic" material model are set up.". Table 3.2 displays the other material properties. The volume pile cannot produce the same force outputs as the embedded pile because of the volume element in the soil material. Therefore, a beam element is introduced at the volume pile's axial axis in order to examine the effects of force. With the exception of the E modulus, which is 10^6 times lower than that of the volume pile material, this beam is configured with the same characteristics as the volume pile (see Table 3.3). (Dao, 2011)

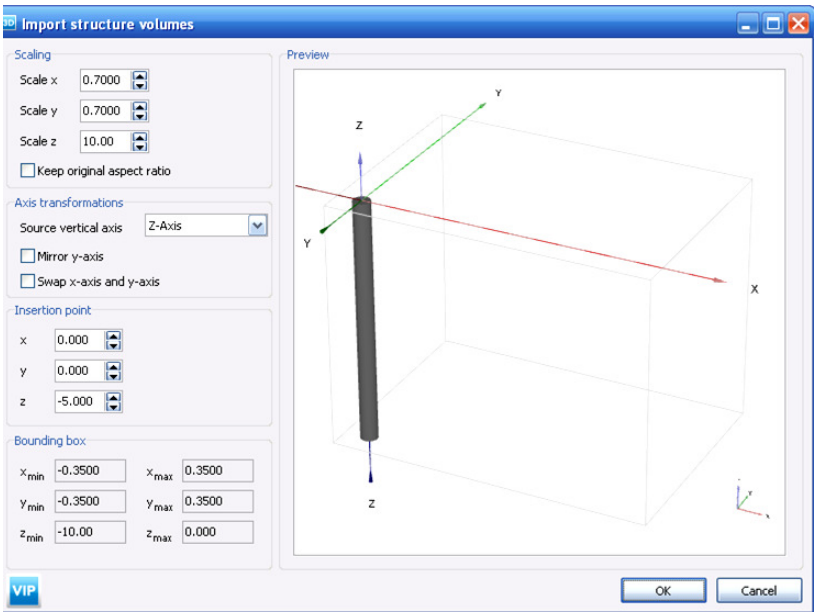

Figure 4.1: Shape and location of volume structure in Plaxis 3D *(Dao, 2011)*

4.3. Generation of the Model

4.3.1. Model Geometry

In this study, the Plaxis 3D FEM program was used to perform numerical modeling on a single pile in stratified soil. A Plaxis 3D volume pile model was used to model the pile. Both the pile's length and diameter affect the model geometry. The cross section of the soil block was pre-defined in the model tab of the project properties window, and the soil is layered. Based on the pile geometry, the limits of the soil contour were defined as the x_{min}, x_{max} and y_{min}, y_{max} . The depth (z-axis) was applied using the "create borehole" button, in this function groundwater table, level can also be selected. The top boundary of the soil layer is at z = 0, and the bottom boundary of the soil layer is a function of pile diameter and its length. Once the soil block was drawn, the soil properties can be assigned to it.

According to (Karthigeyan et al., 2007) static lateral load condition, the soil mass dimension depends on the pile diameter and length. The width of the soil mass was calculated as 40D, where D is the width or pile diameter. When the breadth exceeds 40D, the impact of soil mass on the pile reaction decreases. As seen in Figure 4.4, the height of the soil mass was calculated as L+20D, where L is the pile's length.

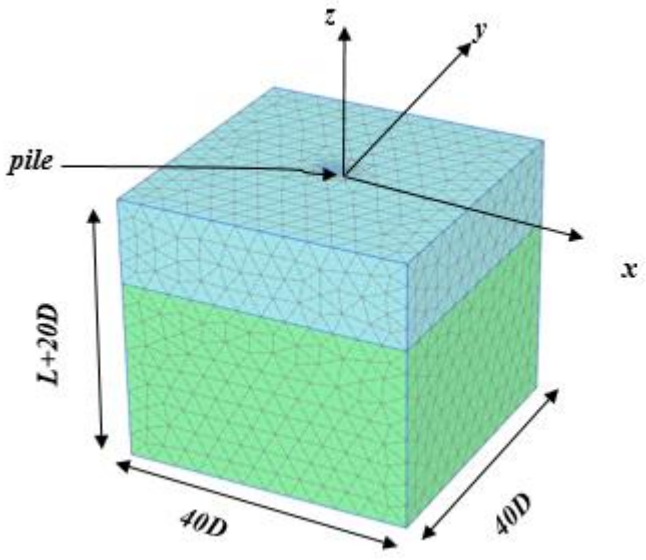

Figure 4.2: 3D finite element mesh for soil mass and location of pile

Table 4.1: 3D FEM model dimensions (design of experiments)

Embedded pile length L(m)	Pile diameter D (m)	Width of soil mass along X (m)	Length of soil mass along Y(m)	Height of soil mass along Z (m)
5	0.6	24	24	17
	0.8	32	32	21
	1	40	40	25
10	0.6	24	24	22
	0.8	32	32	26
	1	40	40	30
15	0.6	24	24	27
	0.8	32	32	31
	1	40	40	35

4.3.2. Model Properties

Finite element analysis software Plaxis 3D was used to investigate how vertical stress affected a pile's lateral response. To perform parametric research, other characteristics should be kept constant while analyzing the effects of altering a specific attribute. The interpretation of parametric study data may be more difficult due to the interplay of several elements. Furthermore, true laterally loaded pile models with all exterior borders will require a substantially greater number of 3D mesh elements, resulting in longer calculation times.

The vertical pile and its characteristics were modeled in all investigations using Plaxis 3D's volume pile option. With this feature, piles might be modeled as structural parts with specific mechanical and stiffness characteristics.

In order to build proper geometry and model of the problem, the boundary size, surface fixity conditions, and mesh generation impacts were explored before thoroughly examining the components affecting the behavior of the pile-soil interaction.

4.3.3. Model Boundary Fixities

The model's soil boundaries must be restricted in both vertical and lateral directions so that the soil's displacement from the lateral load is minimal. Numerous writers proposed various boundary positions in order to reduce the boundary effects in the model. There was no discernible variation in stress and

strain after the horizontal length extent of 40D (40 times the pile diameter) and the vertical depth extent of L+20D (length of a pile plus 20 times its diameter) (Karthigeyan et al., 2007).

As a result, the model's boundaries were positioned sufficiently away from the pile to reduce their impact on the pile's deformations. The model was subjected to three different boundary conditions. Nodes on both lateral boundaries of the model were fixed against horizontal movement($u_x = u_y = u_z = 0$), yet free to move in the horizontal direction. Meanwhile, nodes on the bottom boundary of the model were fixed against all directions($u_x = u_y = u_z = 0$), whereas the top boundary was free to move in all directions as shown in Figure 4.2.

The size and geometry of the model should be selected so that the boundaries are far from the area where calculations are being done and that the stress-strain distributions of the soil are unaffected by geometrical restrictions at the boundaries. However, because three-dimensional studies require significant computing times, this process is inefficient.

The size and geometry of the model, along with the distance to the limitations, were analyzed to determine the optimal dimensions adequate for a precise model. The deflections in the soil were investigated because the model boundaries do not change or interfere with pile resistance.

4.3.4. Mesh Generation

The finite element mesh generation process is carried out following the completion of the soil and structural model's geometry and input parameters. In order to do calculations, the model made up of soil and structural components is divided into volume parts, a process known as mesh generation. Ten-node tetrahedral elements are produced by Plaxis 3D in the mesh procedure of soil volume.

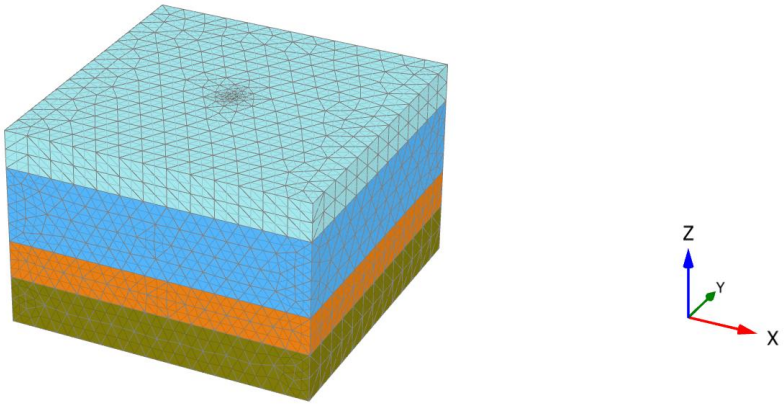

Figure 4.3: Typical mesh connectivity.

The mesh element size can be adjusted using line, cluster, and point refinements in addition to a basic mesh size that spans from extremely coarse to very fine. Extremely fine meshes should be avoided in order to reduce the number of elements and, consequently, the memory use and computation time. Once the mesh is generated, the program cannot insert a new soil cluster or structural element. If a new element or cluster was added to the geometry model, the mesh generation procedure must be repeated using the new input.

4.3.5. Sensitivity Analysis

The model has been divided into components that, as mentioned before, comprise the "finite element mesh" in the finite element computations. The size of the finite element mesh may have an impact on the results. The impact of mesh coarseness and element count on the behavior of laterally loaded pile foundations were investigated using five different finite element meshes. These were achieved by changing their size and quantity while keeping the same material properties and other factors constant. For this reason, the pile head was subjected to a horizontal force of 2548 kN/m2. Both the generated number of elements and the head deflection of a pile are shown in Table 4.2.

Table 4.2: Influence of mesh size on head deflection

Model	Mesh Coarseness	Number of elements	Head deflection (mm)
1	Very Coarse	6062	53.2
2	Coarse	7121	52.2
3	Medium	12146	50.11
4	Fine	25071	49.31
5	Very Fine	59832	48.22

Table 4.2 shows how mesh density affects the head deflection of the pile. Head deflection decreases as the number of elements rises until 12146, when an increase in elements has no appreciable effect on the pile's head deflection, as the image shows. It is possible to deduce that the mesh is convergent with 12146 elements as there is no appreciable change in deflection when the number of elements is increased to 59832. Therefore, model 3 (medium mesh) was used to investigate how vertical load affected the pile foundation's overall lateral reaction.

4.3.6. Calculation Process (Loading Scenarios and Analysis Procedure)

The pile is modeled with a surface at the top. The lateral load is applied as a specified displacement at the surface of the pile head, while the vertical static load is applied as a constant surface pressure, σ_z, on top of the pile. The advantage of employing prescribed displacement rather than a load is that Plaxis 3D allows for the direct extraction of force and displacement from the output. Phase-by-phase calculations are made using Plastic analysis and Stage construction. To investigate the effect of the combined vertical and lateral load on the lateral reaction, the lateral deflection is examined using a node at the top of the pile. The force and displacement. A node at the top of the pile is utilized to examine the lateral deflection in order to study the impact of the combined vertical and lateral load on the lateral reaction. This node, located in the middle of the pile head, is where the force and displacement of the pile are taken from.

First vertical capacity analyses are performed. The vertical capacity is found by applying a vertical surface load at the pile head and loading until failure.

In Plaxis 3D, the construction stages of a finite element model are defined by calculation phases. The calculation phases used for creating the finite element model presented in this chapter are listed below:

The analysis followed a phased approach:

1. Initial Phase: K0 stress generation ($K0=1-\sin\phi'$)
2. Pile Installation: Wished-in-place simulation
3. Loading Phases:
    - ❖ Phase 1: Pure uplift (displacement-controlled to 0.05D mm)
    - ❖ Phase 2: Pure lateral (displacement-controlled to 0.1Dmm)
    - ❖ Phase 3: Combined loading scenarios

An interface was developed in order to establish a positive link between the soil volume and the pile structure. In order to properly describe the interaction between soil and structure, interfaces were joint elements that were added to the surfaces. The contact between a plate (from the pile construction surfaces) and the surrounding soil was simulated using interfaces. It is possible to establish an interface between two soil volumes or next to the plate or geogrid parts. In the model, the interface was created next to the pile plates. The thickness of the interface was zero, which means that the pair of nodes were located with the same coordinates. The interface consists of 16 nodes of quadrilateral shaped

elements. Interface elements are numerically integrated using three Gauss integration points. Figure 4.4 shows the position of the nodes and integration points.

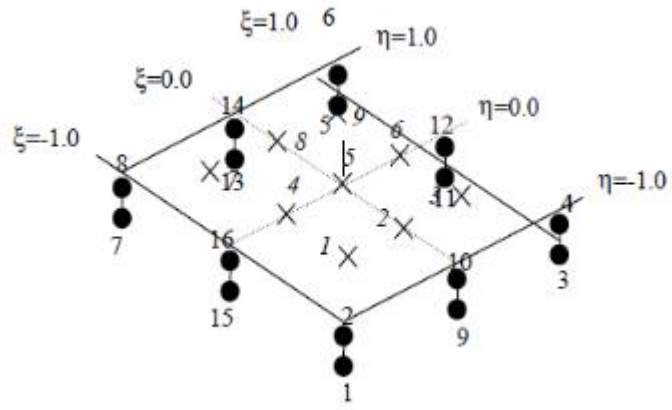

Figure 4.4: Local numbering and positioning of nodes (Ɛ) and integration points (x) of a 16-node interface element (Plaxis 3D, 2021).

Instead of having a single node, the interface elements have pairs of nodes. In a node pair, there is no distance between the two nodes. These interface nodes are designed to accommodate differential displacements between the gapping and slipping node pairs.

The parameter Rinter controls the stiffness and strength of the interface, which can be defined based on the type of study. In situations when the interface should not be less strong than the surrounding soil, a rigid, completely rough soil-structure is employed. These interfaces' strength was determined to be rigid, which is equivalent to Rinter = 1.0. It functions similarly to the neighboring soil element in terms of material qualities. The interface between the soil and the structure was described as absolutely rough in the thin layer element technique.

The following rules are applied to calculate the interface properties from the soil properties in the related data set and value of *Rinter*.

$c_{inter} = c_{soil}$ .....*(4.1)*

$tan\phi_{inter} = tan\phi_{soil}$.....*(4.2)*

Where: c_{inter} –Cohesion of the interface

c_{soil} -Cohesion of the soil

$tan\phi_{inter}$ –Interface friction angle

$tan\phi_{soil}$ –Soil friction angle

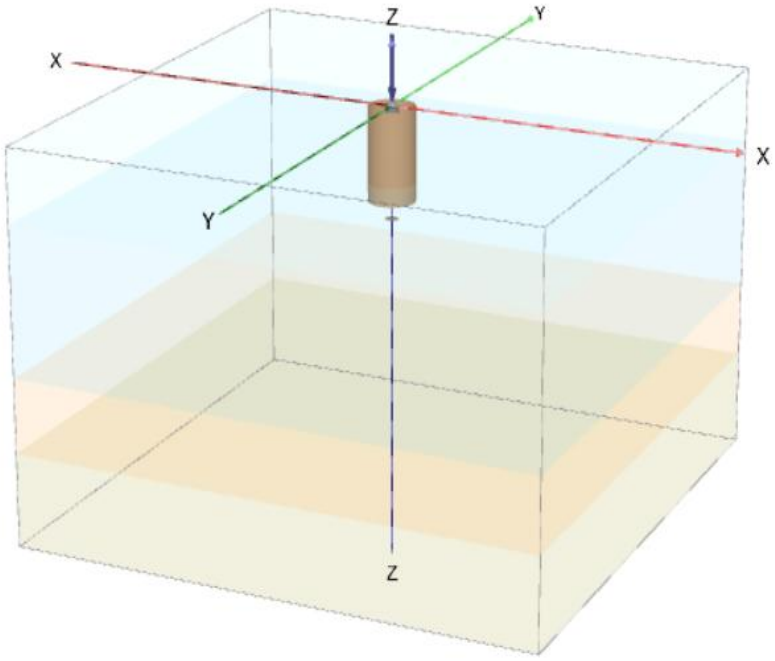

Figure 4.5: Creation of Pile structure and Loads.

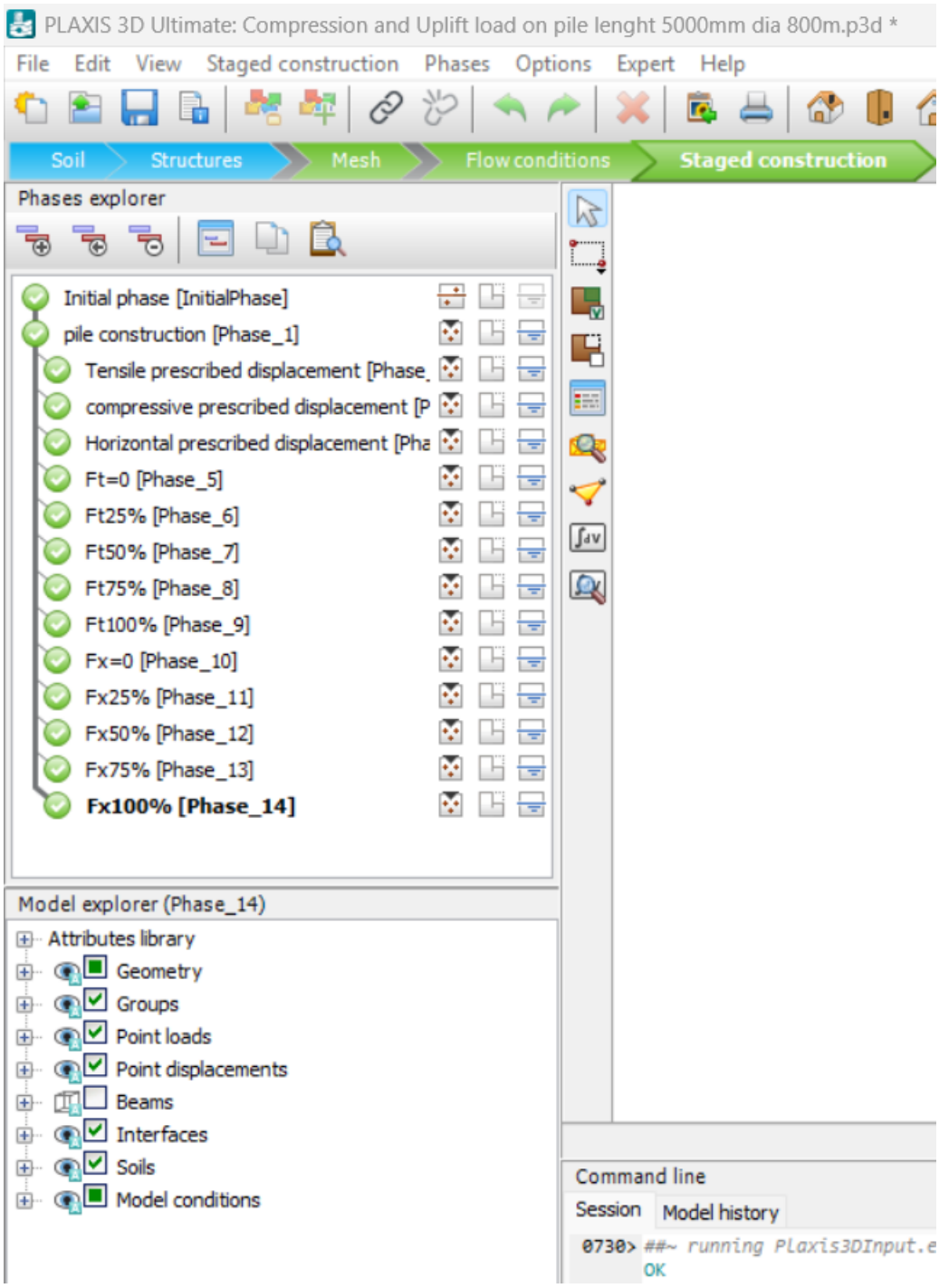

Figure 4.6: Application of load on Pile in different stages

4.4. Validation of Numerical Model

In this study, the lateral response of piles to lateral loads was examined using the finite element method. In this section, the accuracy of the finite element method for evaluating laterally loaded piles is evaluated, and specific finite element details, including pile displacement, are confirmed. Numerous

examples of full-scale lateral pile response to lateral loads have been recorded, according to the literature. In order to compare it with the current study of laterally loaded heaps, it works with a full-scale laterally loaded pile (F. Ismael, 1998). Due to the imperfection of soil data collected from the site and laboratory, certain assumptions are made for the situation of laterally loaded piles embedded in layered media.

This section is used to validate specific details of the finite element, like pile displacement, and to evaluate the accuracy of the finite element approach in evaluating laterally loaded piles. To compare the results from experimental research and finite element analysis, a verification case was developed. Full-scale lateral load tests published by F. Ismael (1998) are included in the comparative case. The well-instrumented soil profiles and attributes are determined by the outcomes of field and laboratory experiments.

Table 4.3: Geotechnical properties of the soil layer

Parameters	Name	Medium dense cemented silty sand layer	Medium dense to very dense silty sand	Pile	Unit
Unsaturated Soil Weight	γ_{unsat}	18	19	25	kNm^{-3}
Saturated soil weight	γ_{sat}	18	19	-	kNm^{-3}
Young's Modulus	E	13000	13000	2.00E+09	kPa
Poisson's Ratio	ν	0.3	0.3	0.15	-
Cohesion	c	20	1	-	kPa
Friction Angle	ϕ	35	45	-	°

In the lateral load case study, a field test on a single pile under lateral stress was conducted to investigate the deflection response of bored piles in cemented sand (F. Ismael, 1998). Each pile was three or five meters in length and 0.3 meters in diameter. This load test was conducted in Kuwait. Shear strength and other effective metrics were used to characterize the surface soil down to a depth of 3.5 meters. To a depth of three meters, the soil profile is composed of a medium-dense layer of cemented silty sand. To the bottom of the borehole, this is covered in medium-to-very-dense silty sand with cemented lumps. After finishing the entire geotechnical model for lateral pile tests, the pile was subjected to the identical load sequence as the pile tests.

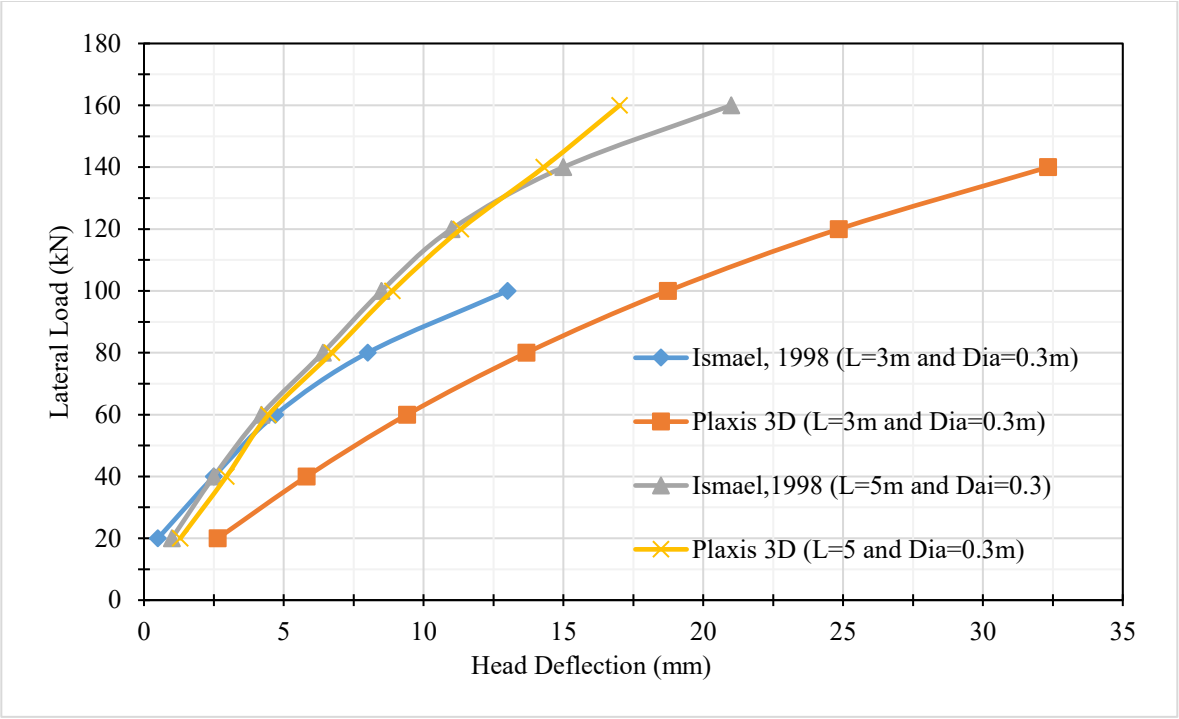

Figure .4.7: Comparison of finite element result with field test data from (F.Ismael, 1998).

The comparison between the finite element result and layered sand field test data is shown in Figure 4.7. The pile with a length of 5m is highly resistance to the lateral load from the second pile length value. Comparable data were obtained between the experimental results of the three piles and the present simulation model. The results obtained from the numerical simulation for a pile of 5m is relatively close with the result obtained from the field test.

5. Results and Discussions

This chapter presents a comprehensive analysis of the numerical investigation results for single piles under pure uplift, pure lateral, and combined loading conditions. The discussion focuses on quantifying the interaction effects, analyzing layer-specific responses, and developing practical design recommendations. The results are organized to systematically illustrate the behavior of three different pile diameters and lengths of (D = 0.6 m, 0.8 m, 1.0 m) and (L=5 m, 10 m, 15 m) respectively.

5.1. Pure Uplift Capacity Analysis

The ultimate uplift capacity (Tu) was determined for each pile diameter by applying a vertical displacement-controlled load at the pile head until a clear failure plateau was reached in the load-displacement curve.

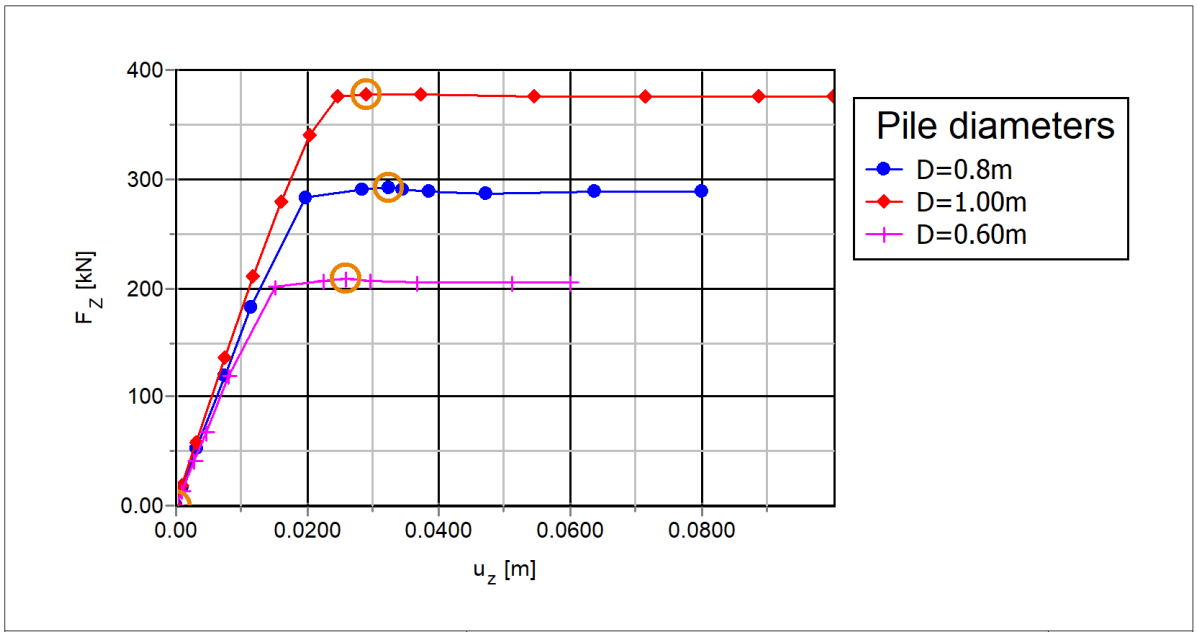

Figure 5.1: Uplift load with vertical displacement of pile with length 5m

Figure 5.1 shows the uplift load (F_z) versus vertical displacement (u_z) for piles of length 5 m with three different pile diameters: 0.6 m, 0.8 m, and 1.0 m.

For all three pile diameters, the uplift load increases with vertical displacement first in a nearly linear manner, indicating elastic mobilization of shaft resistance and soil support.

After approximately $u_z = 0.02 - 0.03\,m$ (20-30 mm), a plateau is reached for all curves where the uplift load reaches ultimate capacity and is nearly constant despite further displacement, indicating failure or full mobilization of shaft resistance.

Ultimate uplift capacities are higher for larger diameter piles:

- D=1.0 m reaches about 378 kN ultimate uplift load.
- D=0.8 m reaches about 292 kN ultimate uplift load.
- D=0.6 m reaches about 208 kN ultimate uplift load.

The initial stiffness, represented by the slope of the early upward curve, also increases with diameter, showing that larger piles resist more even at small displacements. The plateau phases indicate that above a certain level of displacement, additional displacement does not increase the uplift load, simulating the failure of the pile-soil interface or the progressive formation of the failure surface. The steepness of the curve flattening suggests quite a brittle failure mechanism for the smaller piles compared to the slightly more gradual plateau for the large diameter pile.

This chart clearly illustrates the positive effect of rising pile diameter on the initial stiffness and ultimate uplift capacity for a short 5 m length pile:

- Larger diameter piles mobilize greater shaft resistance due to higher surface area and stress distribution in soil.
- The change in behavior from elastic to plastic failure occurs at about the same levels of displacement for all sizes.
- Engineers need to take these diameter-dependent uplift behavior into account when designing piles under tensile loading for appropriate safety margins.

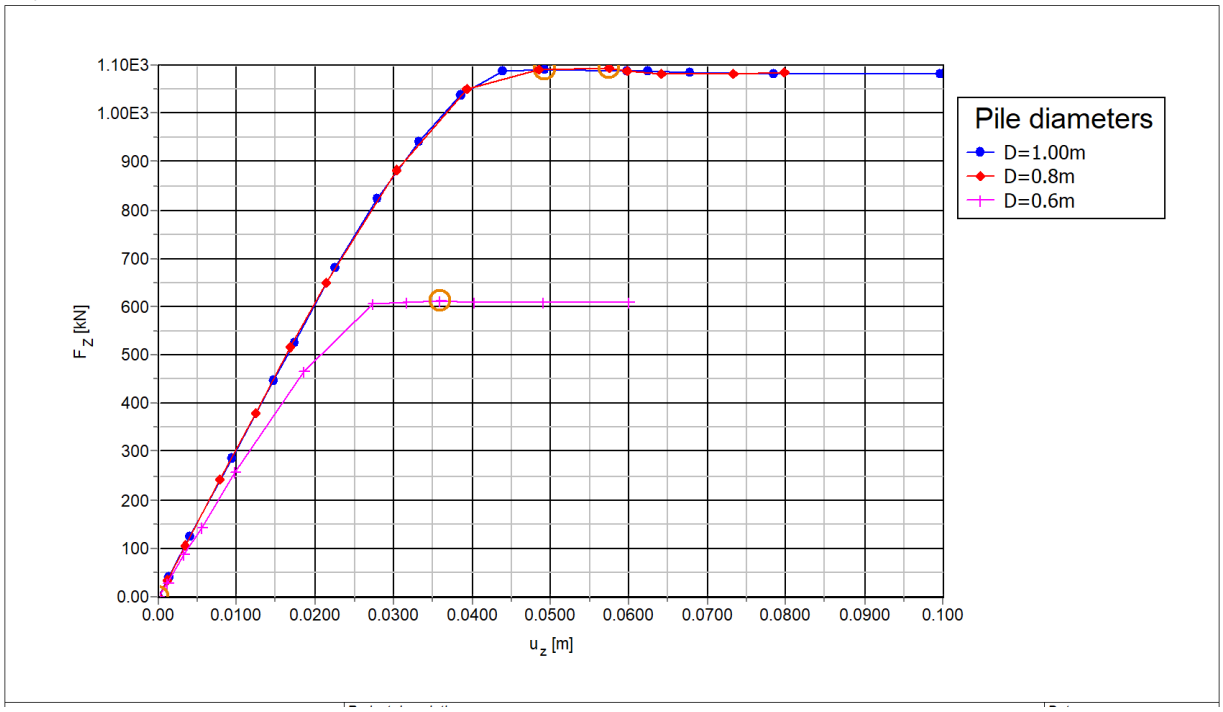

Figure 5.2: Uplift load with vertical displacement of pile with 10m.

The initial parts of all three curves (low displacement region) show approximately linear behavior reflecting the elastic mobilization of pile-soil interface resistance.

For each diameter:

- $D = 1.0\ m$ reaches uplift capacities slightly above 1100kN, plateauing near a displacement of 0.03-0.04 m (30-40 mm).
- $D = 0.8\ m$ reaches uplift capacities just below 1100kN at similar displacements.
- $D = 0.6\ m$ reaches uplift capacity around 600kN, showing a clear plateau after 0.03 m (30mm) displacement.

Notably, the larger piles exhibit a sharper stiffness increase early on with a slightly delayed plateau compared to the smallest diameter, indicating incremental mobilization along the deeper soil shaft.

The data reveals that increasing pile length from 5 m to 10 m roughly triples uplift capacity for the largest pile, illustrating length's significant effect on mobilizing deeper, stronger soil layers. The graphs also show consistent displacement at which ultimate capacity is reached for all diameters (30 to 40 mm), suggesting similar failure surface development mechanics despite size variability.

Interpretation and Engineering Implications

- The clear separation in ultimate capacity for different diameters suggests that pile diameter significantly influences uplift resistance, and thus pile sizing must carefully consider uplift load requirements.
- Longer embedment length allows more effective mobilization of deeper soil strength and interface friction, critical for tension-critical structures.
- The load-displacement relationship highlights elastic and plastic phases useful for capacity design and deformation limit states in pile design codes.
- This Figure demonstrates the necessity to assess both pile length and diameter in uplift capacity predictions to avoid unconservative or overly conservative design.

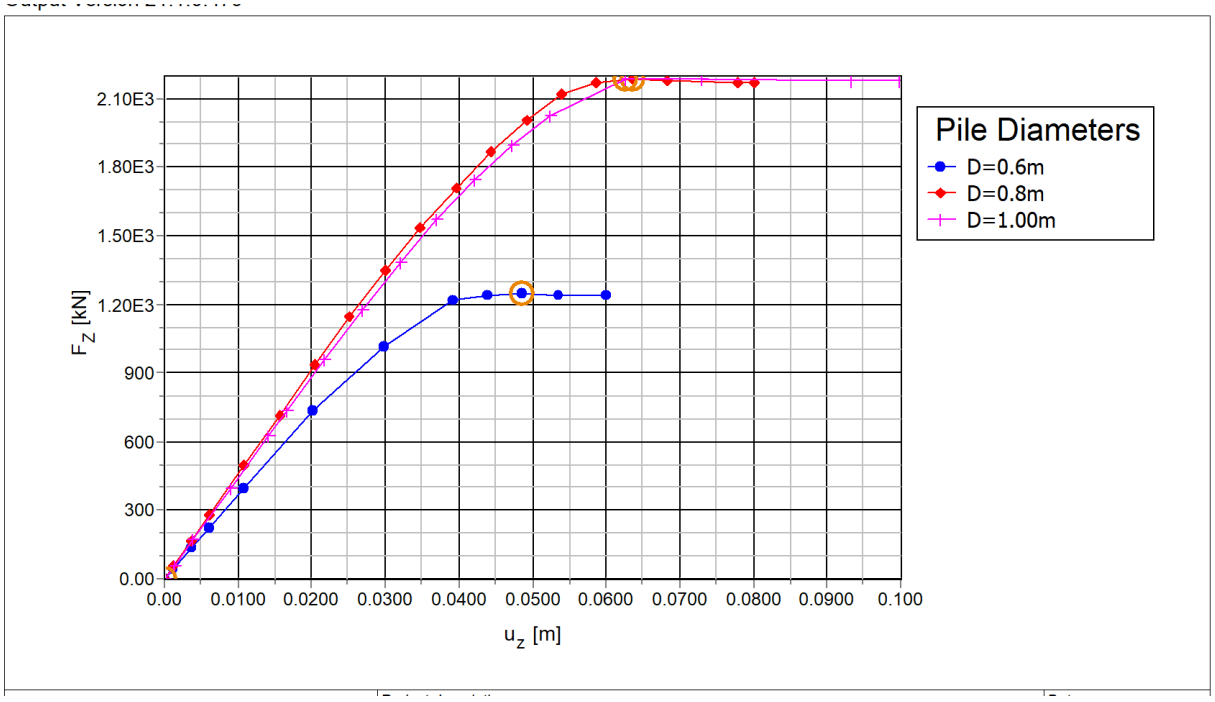

Figure 5.3: Uplift load with vertical displacement of pile with 15m.

The graph shows substantial uplift capacity increases compared to shorter piles (5 m and 10 m) due to the longer embedment length engaging more soil shear strength. Uplift load initially increases nearly linearly with displacement for all diameters, representing elastic mobilization of shaft friction and soil resistance.

Ultimate uplift capacities plateau at significantly higher values:

- For $D = 1.0\ m$, ultimate capacity reaches about 2100 kN.

- For $D = 0.8\,m$, ultimate capacity is slightly lower, very close to $D = 1.0\,m$ (around 2100 kN), suggesting both reach similar capacity levels at this length.
- For $D = 0.6\,m$, ultimate capacity plateaus near 1200 kN, markedly less than the larger diameters.

The displacement at which ultimate capacity is achieved increases slightly with pile diameter, generally occurring around 40 to 60 mm vertical displacement.

The curves for the 1.0 m and 0.8 m diameter piles nearly overlap over the whole range of displacement and load, suggesting that for the chosen soil and pile length, increasing diameter from 0.8 m to 1.0 m yields diminishing returns. The smallest diameter pile (0.6 m) exhibits a noticeably lower load capacity and earlier plateau, indicating less shaft area available for shear mobilization despite the longer embedment.

The initial stiffness (slopes near zero displacement) increases with diameter, consistent with stiffer pile-soil composite behavior.

The elongation of the load-displacement curves before plateauing suggests larger piles sustain higher displacements before failure surface fully develops or soil interface is mobilized.

Interpretation and Significance

- At a 15 m embedment, the uplift capacity is significantly influenced by both pile diameter and length, but the effect of diameter becomes less dominant moving from 0.8 m to 1.0 m.
- The similarity between 1.0 m and 0.8 m piles' capacities indicates soil strength parameters and interface properties could be controlling the capacity ceiling more than geometric increases alone at this scale.
- The data reflects soil-pile interaction saturation, where beyond certain geometry thresholds, soil properties govern capacity limits.
- This graph reinforces the need for balancing pile diameter with soil conditions and length in design to optimize performance and cost.
- Such load-displacement relationships are critical for assessing pile performance under uplift loads, providing insights into elastic stiffness and ultimate capacity for design and safety checks.

This investigation of load-displacement behavior informs both initial design sizing and detailed finite element model validation for long piles under uplift loading. Combining this with lateral and combined load studies yields comprehensive design insights.

5.2. Pure Lateral Load Capacity

The ultimate lateral capacity (Hu) was defined as the load corresponding to a pile head deflection of 10% of the pile diameter (a common geotechnical criterion).

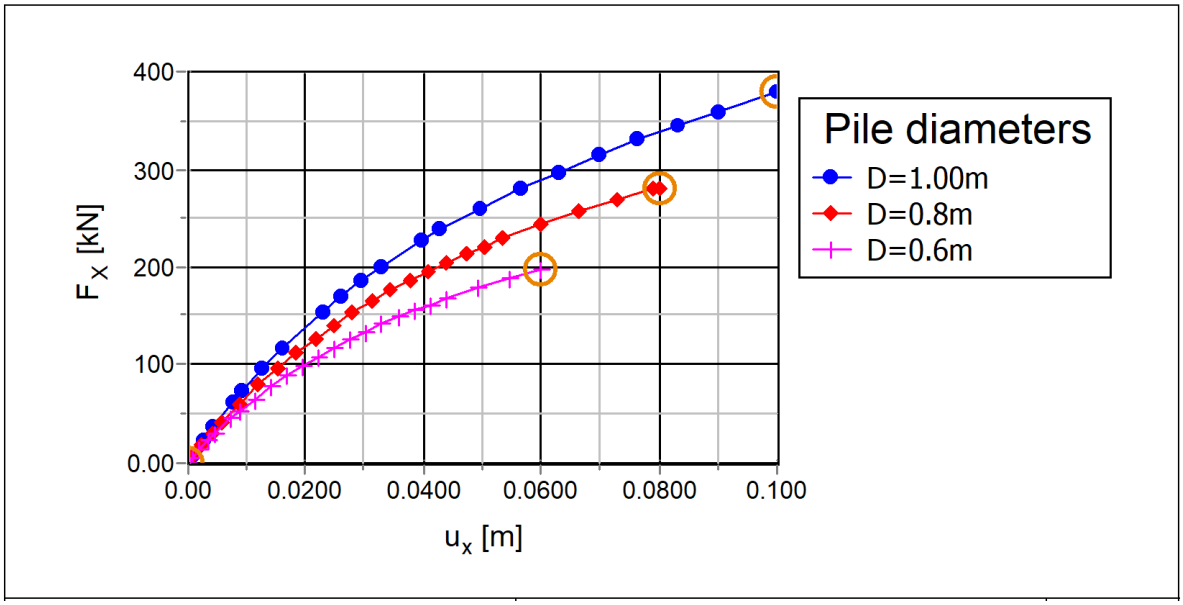

Figure 5.4: Lateral Load vs. Deflection Response for pile length of 5m.

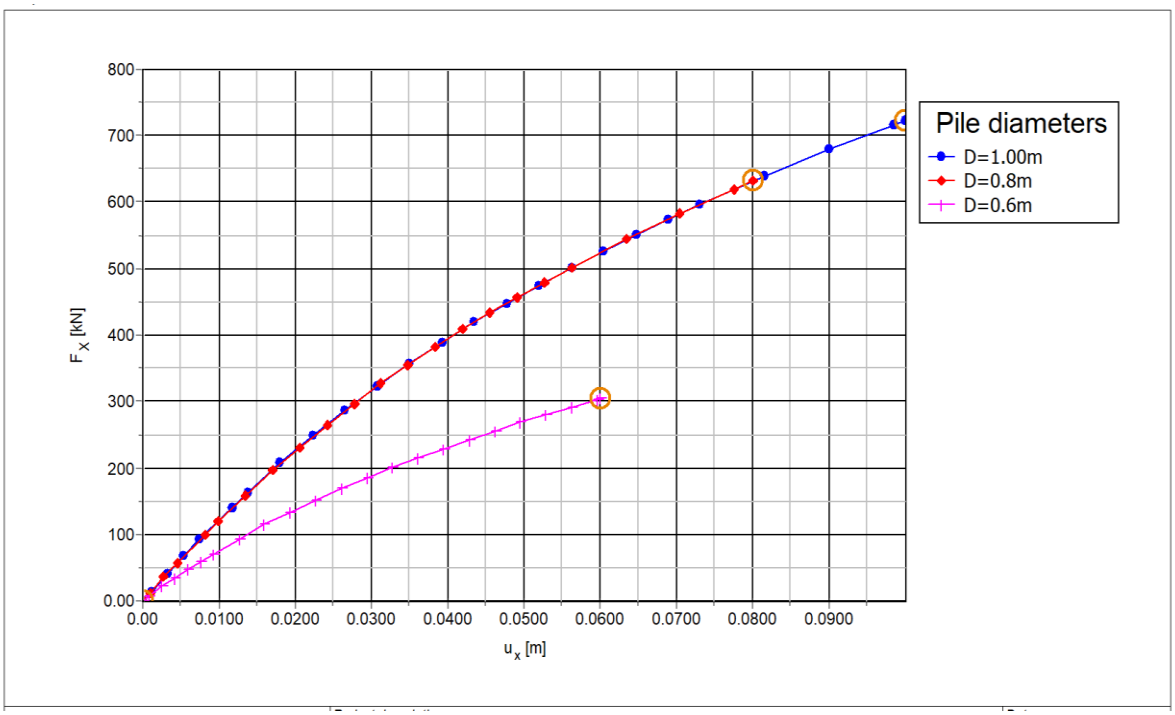

Figure 5.5: Lateral Load vs. Deflection Response for pile length of 10m.

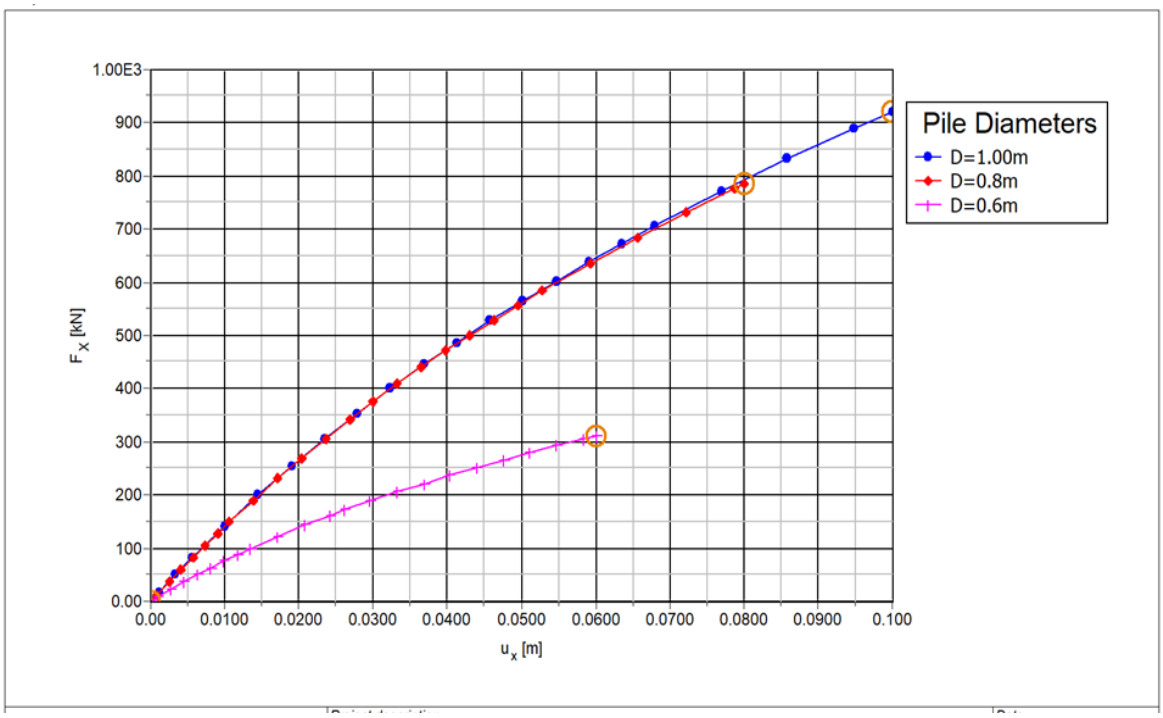

Figure 5.6: Lateral Load vs. Deflection Response for pile length of 15m.

The lateral capacity shows an even more dramatic increase with diameter than the uplift capacity. The Hu for the 1.0m pile is nearly 3 times that of the 0.6m pile. This is because lateral resistance is a

function of the pile's flexural stiffness (EI) and the surrounding soil pressure, both highly dependent on diameter.

5.3. The effects uplift load on the lateral response of piles

For all Figures 5.7 to 5.9, the Variable and Axes:

Curves: Each curve corresponds to a different sustained uplift load ratio (Ft): 0 (no uplift), 0.25Fult, 0.5Fult, and 0.75Fult.

Vertical Axis: Lateral load (Fx), kN.

Horizontal Axis: Lateral pile head displacement (Ux), m (ranging up to about 0.08 m, which is 0.1D for a typical 0.8 m diameter pile).

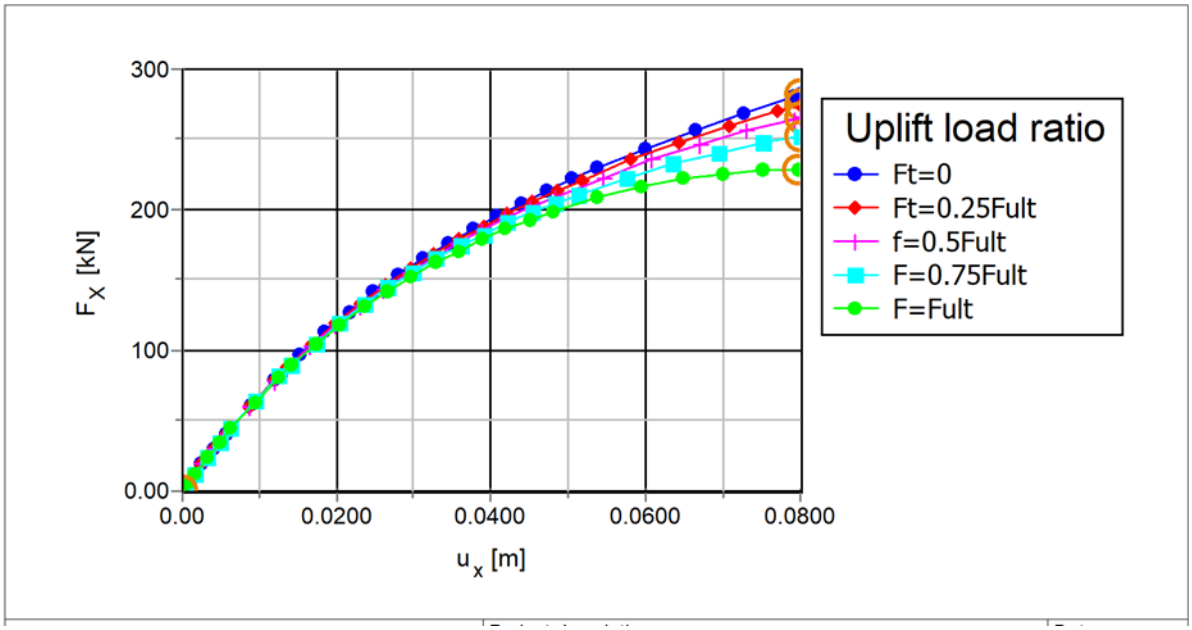

Figure 5.7: Effect of uplift load on lateral load response of pile with length 5 m for pile displacement of 0.1D.

Trend Description

- The **lateral load–displacement** curves clearly show that as the **uplift load ratio** increases from 0 (Ft = 0) to 0.75 Fult, the **lateral capacity (Fx)** at a given displacement decrease.
- At **small displacements (Ux < 0.03–0.04 m)**, the effect of uplift is minor, and all curves almost coincide.
- Once **Ux > 0.04 m**, the divergence between curves becomes more noticeable, indicating an increasing uplift–lateral interaction.

Quantitative Summary at ux = 0.08 m (≈ 0.1D)

Uplift Load Ratio	Lateral Load, Fx (kN)	Reduction wrt No Uplift
Ft = 0 (no uplift)	≈ 300 kN	–
0.25 Fult	≈ 280 kN	≈ 7 % ↓
0.5 Fult	≈ 260 kN	≈ 13 % ↓
0.75 Fult	≈ 240 kN	≈ 20 % ↓

The lateral load capacity decreases by roughly 20 % at high uplift ratios (0.75 Fult), similar in proportional magnitude to larger piles but smaller in absolute load values due to reduced embedment.

Physical Interpretation

- **Interaction Mechanism:**
  Uplift loading induces a loss of normal confining pressure around the pile shaft, reducing the pile–soil frictional strength and the passive resistance mobilized during lateral movement.
- **Progressive Sensitivity:**
  The decrease in lateral load response is mild up to 0.5 Fult but more pronounced beyond that due to nonlinear stress release along the pile–soil interface.
- **Pile Length Effect:**
  A shorter (5 m) pile experiences quicker stress redistribution than a longer one.
  This results in smaller absolute reductions in Fx but faster stiffness degradation near the surface.

Engineering and Design Implications

- **Combined Load Consideration:** Design of short piles must still include uplift–lateral coupling, especially for structures like solar masts and short transmission supports.
- **Serviceability Displacement (0.1D):** Evaluating performance at this displacement better represents service conditions where combined load effects manifest before ultimate failure.
- **Nonlinear Behavior:** The interaction is nonlinear, and simple additive methods (e.g., independent vertical and horizontal checks) underestimate the combined reduction in pile strength.

Generally, Figure 5.7 shows the effect of uplift load on lateral load response of a 5 m pile for pile head displacement of 0.1D. Increasing uplift ratio reduces available lateral load capacity, with a ~20 % reduction observed at 0.75Fult due to reduced confining stress and interface friction along the pile–soil boundary.

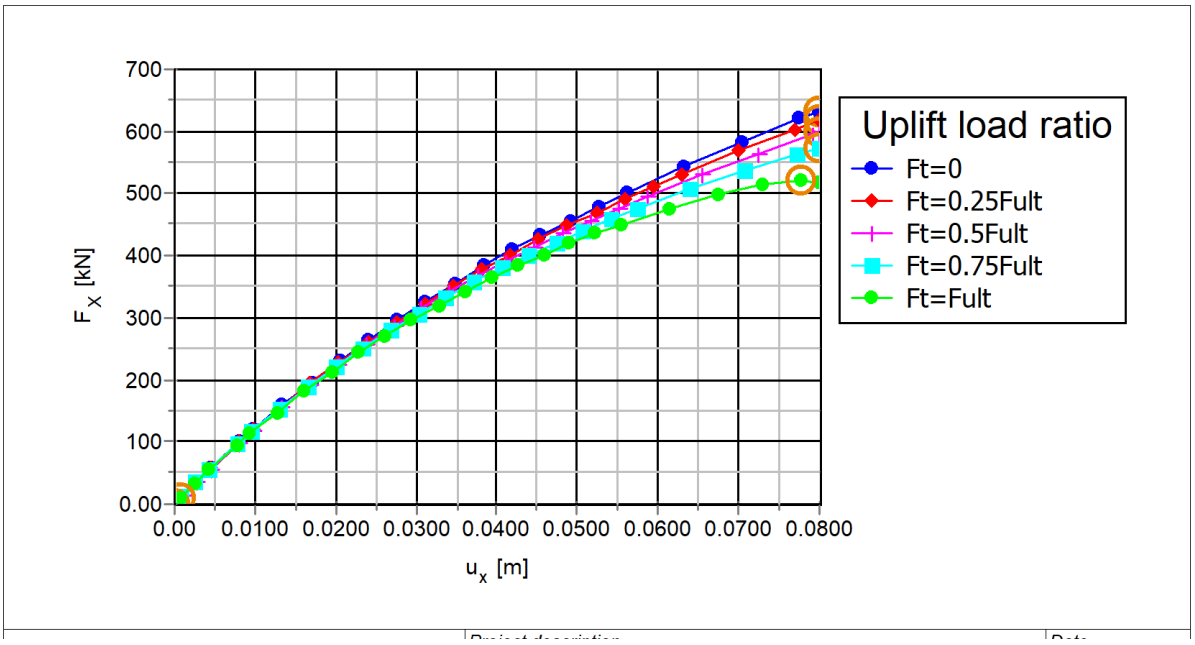

Figure 5.8: Effect of uplift load on lateral load response of pile with length 10m for pile displacement of 0.1D.

Figure 5.8 illustrates the effect of uplift load on the lateral load response of a pile with a length of 10 m, plotted for lateral pile head displacement up to approximately 0.1D (where D is the pile diameter).

Discussion

- Multiple curves represent different uplift load ratios F_t relative to the full uplift capacity (Fult): zero uplift (0), 0.25Fult, 0.5Fult, 0.75Fult, and full uplift (Fult).
- At low lateral displacements, all curves closely coincide—indicating that uplift has minimal initial effect on lateral stiffness.
- As displacement increases toward the design displacement (0.1D), the curves gradually diverge.

- ❖ The lateral load capacity decreases as the uplift ratio increases, with the no-uplift case (blue curve) exhibiting the highest lateral resistance and the full uplift case showing the lowest lateral resistance at the same lateral displacement.
- ❖ The reduction in lateral load capacity with increasing uplift is non-linear, with moderate uplift ratios (0.25–0.5Fult) causing slight decreases and higher uplift ratios (0.75Fult to Fult) producing more pronounced lateral capacity reductions.

Interpretation and Engineering Significance

- ❖ The figure demonstrates the negative interaction between uplift and lateral loading for a 10 m long pile. The increasing uplift load reduces effective normal stress on the soil-pile interface, decreasing shear resistance and lateral capacity.
- ❖ From a design perspective, ignoring these interactions assuming lateral and uplift load capacities independently can lead to incorrect and unconservative capacity predictions.
- ❖ Structures subject to high combined uplift and lateral loading (e.g., foundation piles for transmission towers, offshore platforms) must consider the lowered lateral resistance due to uplift.
- ❖ The results emphasize the importance of combined loading analysis in geotechnical engineering design, encouraging incorporation of interaction factors or nonlinear interaction curves into design standards.

The difference between no uplift and full uplift at service displacement is about 120 kN (nearly 20%), highlighting the significance of the negative interaction. These trends are consistent with established soil–pile interaction theory, confirming that uplift loads reduce lateral pile resistance by diminishing shaft friction and effective support. International design guides and finite-element studies recommend that such interaction effects must be incorporated via interaction diagrams or reduction factors to avoid overestimating pile capacities (ZHU et al,2023).

In general Figure 5.8 underscores the negative, nonlinear effect of sustained uplift on the lateral load-displacement behavior of single piles. Both numerical analysis and engineering practice demand explicit consideration of this interaction for safe, optimized pile design across multiple infrastructure sectors.

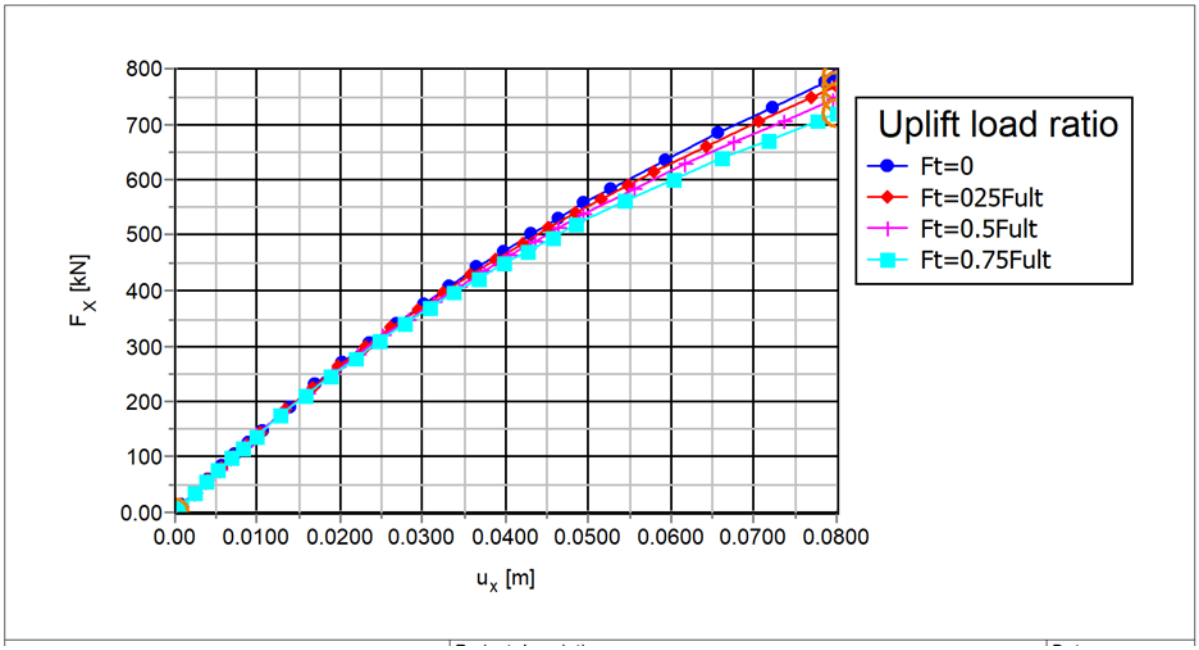

Figure 5.9: Effect of uplift load on lateral load response of pile with length 15m for pile displacement of 0.1D

Figure 5.9 shows the effect of uplift load ratio on the lateral load response of a single pile with a length of 15 m, plotted for lateral displacement up to 0.1D (where, D is the pile diameter).

At low pile head displacements, all lateral load curves (regardless of uplift ratio) are closely grouped, indicating little reduction in initial lateral stiffness due to moderate uplift. As lateral displacement increases, particularly nearing the design limit of 0.1D, divergence between the curves becomes clear: higher uplift ratios correspond to noticeably lower achievable lateral load. At the maximum considered displacement (0.08 m or 0.1D):

- The pile under no uplift (Ft = 0) sustains the highest lateral load.
- Increasing uplift ratio (Ft = 0.25Fult to 0.75Fult) progressively reduces both the slope and the plateau value of lateral resistance.

Physical and Design Interpretation

- **Interaction Effect:**

  The negative interaction becomes more pronounced as uplift load increases. Uplift reduces effective normal stress around the pile shaft, decreasing interface friction and confining pressure. This weakens soil resistance to lateral pile movement, especially along the trailing face leading to reduced lateral capacity.

- **Nonlinearity:**

  The decrease in lateral load capacity is nonlinear; small uplift ratios produce moderate reductions, but reduction accelerates for higher uplift ratios (0.5Fult and above).

- **Structural Implication:**

  For a 15-m pile, this interaction is critical when designing for environments with significant tension (uplift) and lateral loads (e.g., wind, seismic actions). Ignoring the combined effect can lead to unsafe, unconservative designs.

Quantitatively (from Figure 5.9, at $u_x = 0.08\,m$, approximately 0.1D) the drop from no-uplift to 0.75Fult exceeds 12% of the lateral capacity at the design displacement, highlighting the severity of the negative interaction at high uplift levels. These results align with soil-structure interaction theory and field/numerical studies, confirming the reduction in confining stress and lateral resistance under simultaneous uplift. (ZHU et al,2023), (Chen, etal.,2025).

Engineering Significance

- **Capacity Assessment:**

  Lateral pile capacity in combined-action scenarios must be read from the relevant uplift ratio curve, not from the isolated lateral loading curve, to ensure conservative and safe design.

- **Code and Practice:**

  This nonlinear interaction supports the adoption of reduction factors or interaction diagrams in design codes for piles subjected to combined uplift and lateral forces.

- **Site-Specific Design:**

  Where piles are loaded in both actions (e.g., transmission towers, offshore structures), detailed numerical modeling and reference to figures such as 5.9 are essential for robust foundation solutions.

5.4. The effects of lateral load on uplift capacity

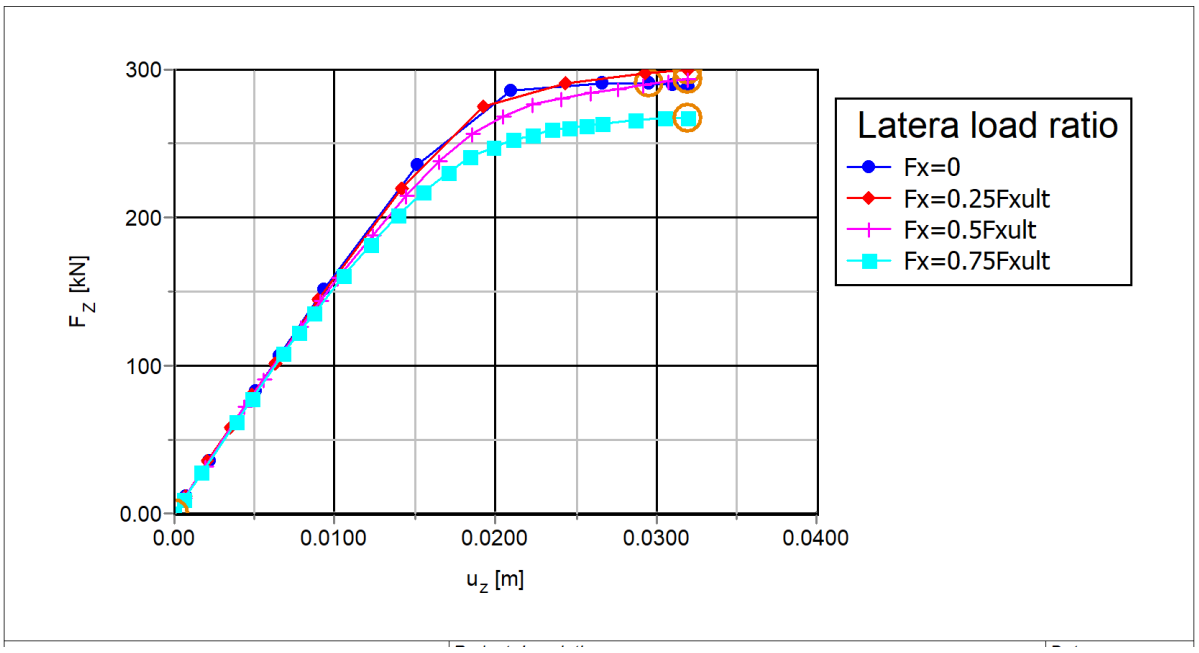

Figure 5.10: Effect of lateral load on uplift capacity of pile with 5m.

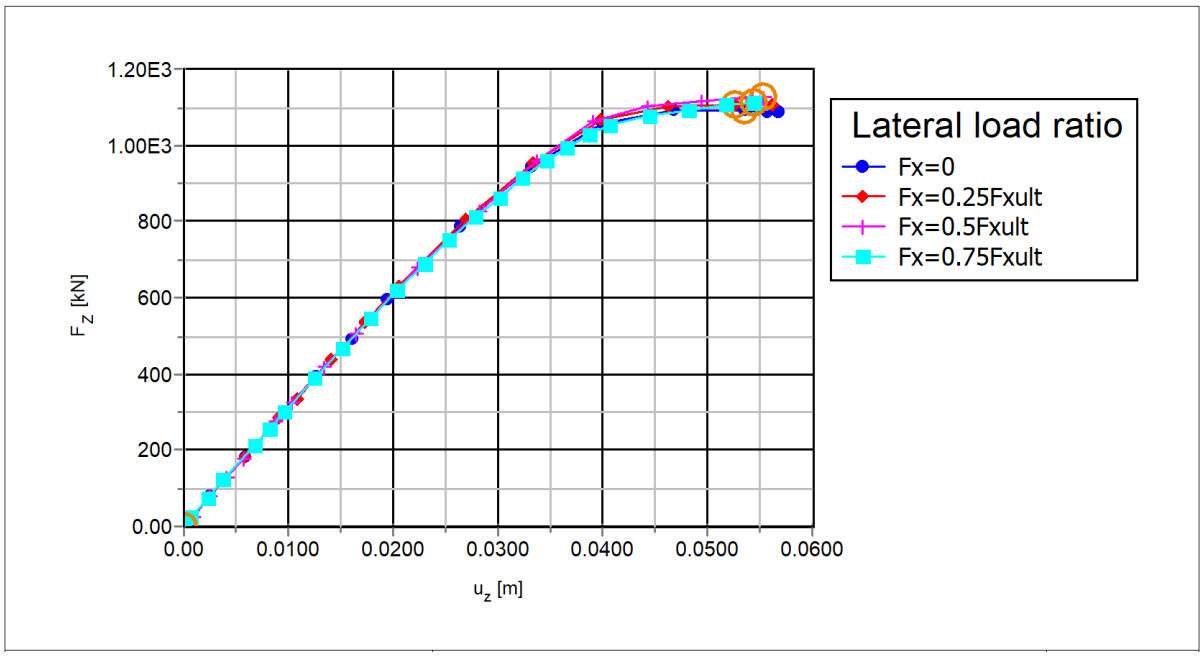

Figure 5.11: Effect of lateral load on uplift capacity of pile with length 10m.

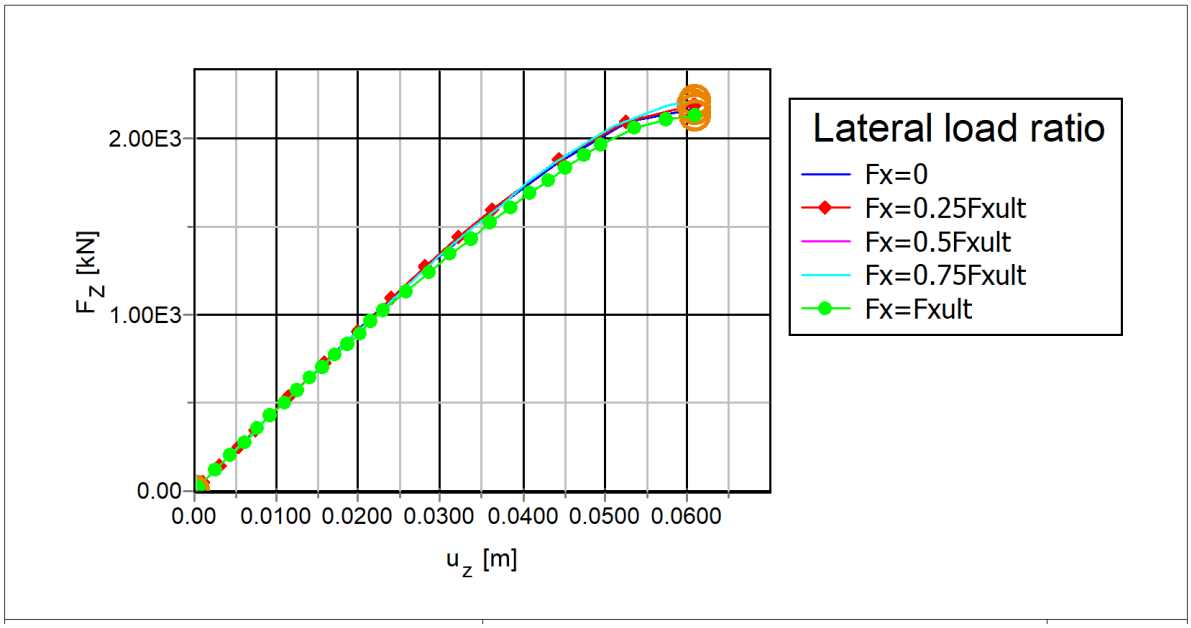

Figure 5.12: Effect of lateral load on uplift capacity of pile with 15m

The strongest and most overall conclusion made from all three graphs is the same: the application of a lateral load does have some significant effect in reducing the ultimate uplift capacity of a pile. This is a fundamental principle of geotechnical engineering, as it illustrates that the lateral and axial behaviors of a pile are interdependent on one another.

The reason for this is that the lateral load induces bending moments in the pile. The bending redistributes to the pile shaft soil pressures. The soil-pile interaction is decreased (even to the point of creating gaps) on one side of the pile, decreasing the level of shaft resistance available to oppose the uplift. Pile capacity is governed by axial tension in combination with bending, rather than pure tension.

Figure 5.9 is the most profound and drastic reduction in uplift capacity under lateral loading. The different lateral load ratio curves are distinctly distinct from one another, and the curve shape itself becomes different. For Fx=0, the pile exhibits a normal ductile response, creating a distinct peak uplift capacity. As Fx increases, the peak uplift capacity declines significantly. Besides, post-peak behavior is more brittle. The collapse is more sudden and at a significantly smaller upward displacement (Uz).

A short pile has a reduced depth of embedment to resist the overturning moment from the lateral load. It behaves more rigidly, and the bending moments in proportion have a greater effect on the entire soil-pile system. The significant loss in capacity and the enhanced brittleness make short piles highly vulnerable to combined loading.

In Figure 5.11 there is also a very clear adverse effect of the lateral load, but one less marked than for the 5m pile. The curves are more clustered, especially under lower values of lateral load ratios.

The ultimate uplift capacity decreases gradually with the increase in the lateral load ratio from 0 to 0.75Fxult. The load-displacement curves are closer to the case of pure uplift (Fx=0), suggesting that there is a more ductile failure mechanism inherited from the 5m pile. There is more flexibility provided by the increased length and a longer lever arm that resists the bending moments due to the lateral load. There is a larger volume of soil that can be mobilized by the pile, resisting the reduction in shaft resistance. Although the capacity remains reduced, the system is more robust.

Figure 5.11 shows the highest most resistant response to lateral loading among the three pile lengths. The reduction in uplift capacity is there but is least significant.

The curves for different lateral load ratios are tightly bunched together. The pile retains a high proportion of its pure uplift capacity even when loaded laterally with a large amount (e.g., Fx=0.75Fxult).

A narrow, long pile is highly flexible and will absorb lateral loads through deflection without causing a failure of adhesion on the entire pile shaft. The bending moments are transferred over a greater depth, and the tip portion of the pile remains highly engaged to contribute towards resisting uplift. This makes longer piles much more efficient under combined load conditions.

Usually,

- Universal Detrimental Effect: Any application of a lateral load always reduces the uplift capacity of a pile regardless of its length.
- Length Dependency is Important: The extent of capacity reduction is heavily dependent on the pile length.
- Short Piles (e.g., 5m): Suffer an extreme capacity reduction and have a tendency towards brittle failure. They are highly sensitive to combined loading.
- Intermediate Piles (e.g., 10m): Exhibit a significant but not too drastic reduction. The system behavior is more adaptable.
- Long Piles (e.g., 15m): Exhibit the best performance, with a moderate reduction in uplift capacity and ductile behavior sustained.

In practice, in design, ignoring the presence of the lateral loads while calculating uplift capacity is non-conservative and risky, especially for short piles. The interaction between the axial (uplift) and the lateral loads must be considered, and the use of longer piles is an effective way to avoid this unfavorable interaction.

Briefly, in the case of this 15 m pile, uplift capacity is little influenced by lateral load over most of the range of displacements, with at best a modest gain at intermediate Fx and no increase (or modest decrease) as Fx approaches its ultimate.

5.4. Effect of Pile Length on Capacity

5.4.1. Uplift Capacity

A comparative interpretation of uplift capacity versus pile diameter and length, based on Figures 5.1, 5.2, and 5.3 data, along with findings.

Table 5.1:Uplift Capacity Trends: Effect of Pile Diameter at Fixed Lengths

Pile Length	D = 0.6 m	D = 0.8 m	D = 1.0 m
5 m	205 Kn	289 kN	375 kN
10 m	608 kN	1,084 kN	1,081 kN
15 m	1,240 kN	2,172 kN	2,175 kN

Table 5.2:Lateral Capacity Trends: Effect of Pile Diameter at Fixed Lengths

Pile Length	D = 0.6 m	D = 0.8 m	D = 1.0 m
5 m	200 kN	280 kN	380 kN
10 m	304 kN	633 kN	723 kN
15 m	311 kN	785 kN	922 kN

Uplift capacity increases approximately linearly with length in shorter piles (5m to 10m), but gains reduce from 10 m to 15 m, indicating mobilization of soil shaft resistance nearing theoretical limits. Longer piles exhibit greater ultimate uplift capacity due to increased embedment providing more shaft surface area and higher effective stresses in deeper layers. Figure 5.1 (conceptual) would show uplift load-displacement curves increasing in ultimate capacity and initial stiffness as length grows. For example, a 0.8m diameter pile's uplift capacity increases from approximately 289 kN (5 m length) to 1,084 kN (10 m) and 2,172 kN (15 m).

5.4.2. Lateral Capacity

Lateral capacity also increases with length, but with diminishing returns beyond 10 m. Maximum bending moments and deflection profiles shift with length; shorter piles tend to behave like cantilevers while longer piles mobilize soil resistance throughout; bending moment peaks move deeper. Longer piles reduce lateral deflections at given load, indicating enhanced stiffness.

5.5. Effect of Pile Diameter on Capacity

5.5.1. Uplift Capacity

Increasing diameter significantly boosts uplift capacity due to increased cross-sectional area and greater shaft surface perimeter. For a 15 m pile length, uplift capacity rises from 1240 kN at 0.6 m diameter to 2172 kN at 0.8 m and up to 2175 kN at 1.0 m diameter. Larger diameters enhance interface area and mobilize more shear resistance on soil-pile interface.

5.5.2. Lateral Capacity

Lateral capacity increases with diameter but less pronounced than uplift because bending stiffness scales with D^4 but soil resistance governs lateral failure more than pile stiffness. Larger piles show reduced lateral deflections and delayed plastic hinge formation.

Variation in pile geometry changes the mobilization of soil resistance:

Longer piles engage deeper, stronger soil layers contributing disproportionately to uplift capacity due to higher overburden pressure and shear strength. Increased shaft area from larger diameters boosts available shear resistance for both uplift and lateral loads. Interface reduction factors influence magnitude but remain consistent across geometries, emphasizing geometry's fundamental role in available resistance.

Failure Mode Evolution with Pile Geometry

Shorter/smaller piles tend to fail via localized shear with early plastic hinge formation near the surface. Longer/larger piles allow for wider plastic zones forming along shaft, with failure surfaces deepening and becoming more complex under combined loading. This alters bending moment distribution, shear strain development, and stress pathways within soil. Designers should apply geometry-dependent capacity factors to improve safety and economy.

6. CONCLUSIONS AND RECOMMENDATIONS

6.1. Conclusions

The main objective of this study was to investigate the behavior of piles subjected to uplift and lateral load in layered soils. The effect of uplift loads on the performance of laterally loaded piles was explored through the application of numerical modeling techniques. The numerical simulations were executed utilizing the advanced computational software PLAXIS 3D, and parametric analysis, incorporating a range of pile diameters and lengths. The outcomes pertaining to the lateral capacities of the piles were ascertained and contrasted for piles experiencing solely lateral loads versus those subjected to a combination of uplift and lateral loads across multiple vertical load scenarios corresponding to 25%, 50%, 75%, and 100% of the ultimate load capacity of the pile. From this comparative analysis, the following conclusions can be drawn:

- The independent analysis of uplift and lateral pile capacity, as commonly practiced, is fundamentally non-conservative and can lead to unsafe designs or uneconomical solutions for piles subjected to combined loading.
- Pile diameter significantly influences both capacity and failure mechanisms, with lateral capacity showing greater sensitivity to diameter changes compared to uplift capacity.
- A strong negative interaction exists between uplift and lateral loading, with combined capacity reductions of up to 12% when lateral loads reach 75% of capacity.
- The developed interaction diagrams provide practical design tools that account for these complex interactions.
- Both uplift and lateral capacities increase with pile length and diameter, with diminishing returns occurring as pile dimensions grow.
- Longer piles resist lateral loading more effectively by distributing bending moments deeper, mitigating normal stress reduction that harms uplift capacity.
- Larger diameters provide substantial uplift capacity gains by increasing interface area and pile stiffness, but lateral gains are less pronounced comparatively.
- The nonlinear uplift-lateral interaction is consistent across pile sizes, but intensity of capacity reduction varies; hence, geometric parameters must be incorporated in design interaction methods.

6.2. Recommendations

The results of this study will be helpful in developing a better insight into the behavior of single pile foundations and will go a long way in assisting the design and analysis of such a structure with caution.

- Adopt Interaction Analysis: Geotechnical design codes and practices in Ethiopia should be updated to mandate the consideration of combined loading effects for piles supporting tall buildings, towers, and bridge piers
- Consider pile length and diameter explicitly in estimating uplift and lateral capacities before applying interaction formulas.
- Favor Slender Piles: In scenarios with significant combined loads, designers should prioritize the use of longer, more flexible piles over shorter, stiffer ones to mitigate adverse interaction effects.
- Use geometry-sensitive interaction charts or formulas to avoid unconservative designs.
- Prioritize deeper soil investigation for longer piles and interface condition verification for larger diameter piles.
- Use Interaction Diagrams: The interaction diagrams developed from this study (or similar project-specific ones) should be incorporated into the design process to ensure safety and efficiency
- Account for installation techniques that may alter interface behavior especially important as pile surface area grows with diameter and length.

Future Work

- Extending analysis with cyclic and dynamic loadings for fatigue and seismic resilience evaluation.
- Inclined (Raked) Piles: Explore the behavior of raked piles under combined loading, which are often used to resist lateral forces.
- Develop family of interaction charts generalized by pile geometry embedded in software design tools for routine application.
- Pile Group Effects: Investigate the interaction effects within pile groups, where the response of one pile under combined loads can influence its neighbors

References

A.M.Trochanis, J.Bielak and P.Christiano. (1991). Three-dimensional nonlinear study of piles. *J. Geotech. Eng, 117*(3), 429–447.

Alasadi A. A. and Mustafa F. S.,. (2022). Numerical Analysis for the Response of Skirt Circular Shallow Footing Resting on Sandy Soil under vertical loads,. *"Kufa J. Eng.,, 13*(2), 16–27.

B .McClelland and J. A. Jr.Focht. (1958a). *Soil modulus for laterally loaded piles.*

B.B.Broms. (1964a, b, 1965). Design of laterally loaded piles. *J. Soil Mechanics and Foundations Division, ASCE, 91*(SM3), 79-99.

B.Hansen, J. (1961). The ultimate resistance of rigid piles against transversal forces. *Bulletin, Danish Geotechnical Institue, Copenhagen, 11*, 5-9.

Basu et al. (2008).

Bowles, J. E. (1996). *Foundation Analysis and Design* (5 ed.). McGraw-Hill Companies, Inc.

Briaud, J.-L. (2013). *Geotechnical Engineering: Unsaturated and Saturated Soil.* New Jersey Hoboken : John Wiley & Sons, Inc.

C.Desai and G.Appel. (1976). 3-D analysis of laterally loaded structures. *Proceedings of the 2nd International Conference on Numerical Methods in Geomechanics*, (pp. 405–418). Blacksburg.

C.Reese, L. (1986). *Behavior of Piles and Pile Groups Under Lateral Load.* Washington D.C: Federal Highway Administration.

D.A. Brown and C.F. Shie. (1990,1991). Three dimensional finite element model of laterally loaded piles. *Comput. Geotec, 10*(1), 59–79.

D.A.Brown,M. Kumar,et al. (1989). PY curves for laterally loaded piles derived from three-dimensional finite element model. Numerical models in geomechanics. *Numog III. Proceedings of the 3rd International Symposium Held in Niagara falls*.

D.Douglas and E.Davis. (1964). The movement of buried footings due to moment and horizontal load and the movement of anchor plates. *Geotechnique, 14*(2), 115–132.

Dao, T. (2011). *Validation of PLAXIS Embedded Piles* . Delft University of Technology .

E.A.Dickin and R.B.Nazir. (1999). Moment-carrying capacity of short pile foundations in cohesionless soil. *Geotechnical and Geoenvironmental Engineering ASCE, 125*(1), 1-10.

E.Barber. (1953). Discussion to paper by SM Gleser. *154*, pp. 96–99 .

F.Ismael, N. (1998). Lateral loading tests on bored piles in cemented sands. *Proceedings of the 3rd International Geotchnical Seminar on Deep Foundation on Bored and Auger piles. 3rd*, pp. 137-144. Belguim: Ghent.

F.Scott, R. (1981). *Foundation Anaysis.* Prentice-Hall, Engel Wood Cliffs, NJ.

Fakher N. and Fakhruldin M.,. (2021). Experimental study of relative density effect on bearing apacity of sand reinforced with geogrid,. *Kufa J. Eng.,, 12*(2), 46–55.

H.G.Poulos. (1971a,b). Behavior of laterally loaded piles. *Journal of Soil Mechanics and Foundation, 97*(5), 711-751.

H.G.Poulos. (1973). Analysis of piles in soil undergoing lateral movement. *Journal of Soil Mechanics and Foundation Division, 99*(5), 391–406.

H.G.Poulos and E.H.Davis. (1980). *Pile Foundation Analysis and Design.* New York: Wiley and Sons.

H.G.Poulos and T.S.Hull. (1989). The role of analytical mechanics in foundation. *Foundation Engineering, Current Principals and Practices.*

H.Matlock and L.C.Reese. (1960). Generalized solutions for laterally loaded piles. *Journal of Soil Mechanics and Foundations Division, 86*(5), 63–94.

Hencher, S. (2012). *Practical engineering geology.* New York: CRC Press.

J.R.Peng, M.Rouainia,and B.Clarke. (2010). Finite element analysis of laterally loaded fin piles. *Comput. Struct, 88*(21), 1239–1247.

K.Yang and R.Liang. (2006). A 3D FEM model for laterally loaded drilled shafts in rock. *Int. GeoCongress 2006@ sGeotechnical Engineering in the Information Technology Age*, 1–6.

Ken Fleming Ken, Austin Weltman,Mark Randolph and Keith Elson. (2009). *Piling Engineering* (3rd ed.). London and New York: Taylor & Francis.

Kranthikumar A., Sawant V. A., and Shukla S. K.,. (2016). Numerical modeling of granular anchor pile system in loose sandy soil subjected to uplift loading. *Int. J. Geosynth. Gr. Eng.,, 2*, 1–7.

Lymon C. Reese and Hudson Matlock. (1956). Nondimensional solutions for laterally loaded piles with soil modulus assumed proportional to depth. *Proceedings of the VIII Texas Conference on Soil Mechanics and Foundation Engineering.* Austin: University of Texas.

Lymon C.Reese and William F.Van Impe. (2011). *Single Piles and Pile Groups under Lateral Loading.* CRC Press Taylor & Francis Group Boca Rotan.

M.A.Biot. (1937). Bending of an infinite beam on an elastic foundation. *Journal of Applied Mechanics, 2(3)*, 165–184.

M.Ahmadi and S.Ahmari. (2009). Finite-element modelling of laterally loaded piles in clay. *162*(3), 151–163.

M.Budhu and T.G.Davies. (1987,1988). Nonlinear analysis of laterality loaded piles in cohesionless soils. *Canadian Geotechnical Journal, 24*(2), 289–296.

M.F.Randolph. (1981). The response of flexible piles to lateral loading. *Geotechnique, 31*(2), 247–259.

M.Faruque and C.Desai. (1982). 3-D material and geometric nonlinear analysis of piles. *Proceedings of the Second International Conference on Numerical Methods in Offshore Pilling*, 553–575.

M.Hetenyi. (1946). *Beams on Elastic Foundation.* The University of Michigan Press.

M.Jamiolkowski and A.Garassino. (1977). Soil modulus for laterally loaded piles. *In Proceedings of the Specialty Session 10, Ninth International Conference on Soil Mechanics and Foundation Engineering*, (pp. 43-58). Tokyo.

M.Mardfekri, P.Gardoni and J.M. Rosset. (2013). Modeling laterally loaded single piles accounting for nonlinear soil-pile interactions. *J. Eng, 3*, 1-7.

M.Wood, D. (1990). *Soil Behaviour and Critical State Soil Mechanics.* New York: Cambridge University Press.

Malhotra H. and Singh S. K. (2022). Effect of load inclination on the uplift capacity of the granular anchor pile foundation in cohesive soil. *Arab. J. Geosci., 15*(11), 1088.

P, S. R. (2020). Pile Settlement Induced From Soil Movement Due To Breakdown Of Retaining Wall. *Acta Polytech, 60*(4), 338–348.

P.K.Banerjee and T.G Davis. (1978). The behaviour of axially and laterally loaded single piles embedded in non-homogeneous soils. *Geotechnique, 28*, 309–326.

P.Kavitha, K.Beena and K.Narayanan. (2016). A review on soil–structure interaction analysis of laterally loaded piles. *Innov. Infrastruct. Solut, 1*, 1-15.

P.W.Rowe. (1956). The single pile subject to horizontal force. *Géotechnique, 6*(2), 70-85.

R.B.J. Brinkgreve and W. Broere. (2006). *Plaxis 3D Foundation Reference Manual Version 1.5.* DELFT, Netherlands.

R.D.Mindlin. (1936). Force at a point in the interior of a semi-infinite solid. *Journal of Applied Physics, 7*(5), 195–202.

R.Tuladhar, H. Mutsuyoshi and T.Maki. (2013). Numerical modelling and full-scale testing of concrete piles under lateral loading. *Aust. J. Struct. Eng, 14*(3), 229–242 .

Reddy K. Madhusudan and Ayothiraman R.,. (2015). Experimental studies on behavior of single pile under combined uplift and lateral loading. *J. Geotech. geoenvironmental Eng., 141*(7), 4015030.

S. Karthigeyan, V. V. G. S. T. Ramakrishna and K. Rajagopal. (2007). Numerical investigation of the effect of vertical load on the. *Journal of Geotechnical and Geoenvironmental Engineering, Vol. 133, No. 5, .*

Sawwaf, M. E. (2006). Lateral Resistance of Single Pile Located Near Geosynthetic Reinforced Slope. *Geotechnical and Geoenvironmental Engineering*.

Shamsher Prakash and Hari D. Sharma. (1990). *Pile foundations in engineering practice.* John Wiley & Sons, Inc.

Spagnoli G. and Tsuha C. de Hollanda Cavalcanti. (2020). A review on the behavior of helical piles as a potential offshore foundation system. *Mar. Georesources Geotechnol, 38*(9), 1013–1036.

Stroud, M. A. (1974). The Standard Penetration Test in Insensitive Clays and Soft Rocks. *Proceedings of the European Symposium on Penetration Testing*, *2*, pp. 367-375. Stockholm.

T.Davies and M.Budhu. (1986). Non-linear analysis of laterally loaded piles in heavily overconsolidated clays. *Geotechnique, 36*(4), 527–538.

Terzaghi, K. (1955). Evaluation of coefficient of subgrade reaction. *Geotechniques, 5(4)*, 297-326.

W.R.Spillers and R.D.Stoll. (1964). Lateral response of piles. *Journal of Soil Mechanics and Foundation Division, 90*(6), 1–10.

Yit-Jin Chen,Mary Abigail Jos,Anjerick Topacio and Kai Wang. (2025). Uplift Capacity and Displacement of Pre-Bored PC Piles in Undrained Soils. *nternational Journal of Engineering and Technology Innovation, 15*(3), 300-313. doi:doi.org/10.46604/ijeti.2024.14597

Z.Yang and B.Jeremi. (2005). Study of soil layering effects on lateral loading behavior of piles. . *Geotech. Geoenviron. Eng, 131*(6), 762–770 .

ZHU, Ke-wen; YU, Jian; and HUANG, Mao-song . (2023). "Upper bound analysis of uplift piles in saturated". *Rock and Soil Mechanics, 44*(7), 1995−2004. doi:10.16285/j.rsm.2022.6185

APPENDICES

The appendices include the following

- Appendix A: Soil profile from Geotechnical Investigation
- Appendix B: Uplift capacity analyses
- Appendix C: Lateral response

Appendix A: Soil profile from Geotechnical Investigation

Table A-1: Description of strata and corrected SPT blow count

BH No. (Location)	Depth (m)	SPT N-value	Layer Description
BH-1	2.00 – 2.45	2/3/4	Medium stiff, dark grey, Fat CLAY soil.
	4.00 – 4.45	3/4/6	Stiff to very stiff, light grey, Elastic SILT/ Fat CLAY soil.
	6.00 – 6.45	4/6/7	
	8.00 – 8.45	5/6/8	
	10.00 – 10.45	6/8/9	
	12.00 – 12.45	5/6/7	
	14.00 – 14.45	5/6/8	Stiff, light brown, Elastic SILT with sand soil.
	16.00 – 16.45	5/7/8	Stiff, light brown, Elastic SILT with sand/ Sandy SILT soil.
	18.00 – 18.45	7/9/10	Very stiff to hard, light grey, Lean CLAY with sand/ SILT soil.
	20.00 – 20.45	R	
	22.00 – 22.45	R	
	24.00 – 24.45	R	
BH-2	2.00 – 2.45	3/4/5	Stiff, dark grey, Fat CLAY soil.
	4.00 – 4.45	4/5/5	Stiff to very stiff, light grey, Elastic SILT/ Fat CLAY soil.
	6.00 – 6.45	5/6/7	
	8.00 – 8.45	6/8/8	
	10.00 – 10.45	6/6/8	
	12.00 – 12.45	5/7/9	Very stiff, light brown, Sandy SILT soil.
	14.00 – 14.45	6/8/10	Very stiff, light grey, SILT with sand soil.
	16.00 – 16.45	R	Hard, light grey to dull white, SILT with sand/ Lean CLAY with sand/ Silty GRAVEL with sand/ SILT/ Sandy Fat CLAY soil.
	18.00 – 18.45	R	

BH No. (Location)	Depth (m)	SPT N-value	Layer Description
	20.00 – 20.45	R	
	22.00 – 22.45	R	
	24.00 – 24.45	R	

Appendix B: Uplift capacity analyses

Table B. 1: Uplift capacities of pile with length 5m

T= 0 (Pure uplift load), d=0.6m		T= 0 (Pure uplift load), d=0.8m		T= 0 (Pure uplift load), d=1.0m	
Uplift laod(kn)	Vertical displacement(mm)	Uplift laod(kn)	Vertical displacement(mm)	Uplift laod(kn)	Vertical displacement(mm)
0.00	0.00	0.00	0.00	0.00	0.00
13.54	0.89	17.32	1.04	19.31	1.07
40.60	2.68	51.95	3.13	57.93	3.20
66.98	4.47	119.57	7.30	135.14	7.46
118.16	8.04	183.03	11.48	210.10	11.72
200.61	15.20	282.11	19.83	278.45	15.98
207.39	22.35	290.83	28.18	341.11	20.25
207.70	25.92	291.71	32.35	376.65	24.52
206.61	29.50	290.52	34.44	377.93	28.79
204.71	36.65	288.38	38.61	377.56	37.33
204.65	50.95	287.15	46.96	375.37	54.42
205.10	60.00	287.75	63.65	374.97	71.51
		288.68	80.00	374.93	88.59
				374.94	99.95

Table B. 2:Uplift capacities of pile with length 10m

T= 0 (Pure uplift load), d=0.6m		T= 0 (Pure uplift load), d=0.8m		T= 0 (Pure uplift load), d=1.0m	
Lateral laod(kn)	Horizontal displacement(mm)	Lateral laod(kn)	Horizontal displacement(mm)	Lateral laod(kn)	Horizontal displacement(mm)
0.00	0.00	0.00	0.00	0.00	0.00
7.47	0.84	11.86	0.89	14.08	1.06
21.50	2.52	35.27	2.68	41.59	3.18
34.54	4.20	57.43	4.46	67.63	5.30
47.10	5.87	100.08	8.03	92.72	7.42
59.23	7.55	120.35	9.81	140.68	11.66
71.05	9.23	159.18	13.38	163.14	13.78
93.52	12.59	196.11	16.94	206.81	18.02
114.39	15.94	231.54	20.51	248.03	22.26
133.74	19.30	265.09	24.08	286.36	26.49
151.87	22.65	296.51	27.64	322.38	30.73
168.99	26.01	326.64	31.21	356.82	34.97
185.07	29.36	355.59	34.77	388.92	39.20
200.28	32.72	382.81	38.34	419.39	43.44
214.90	36.07	408.88	41.90	447.93	47.68
228.94	39.43	433.55	45.47	475.30	51.92
242.41	42.78	457.13	49.04	501.74	56.16
255.48	46.14	479.98	52.61	527.12	60.39
268.13	49.50	502.20	56.18	551.49	64.63
280.27	52.85	544.27	63.31	574.73	68.87
291.85	56.20	583.44	70.44	597.20	73.10
302.96	59.56	620.31	77.57	639.91	81.57
304.37	60.00	632.03	79.93	679.66	90.04
				716.86	98.50
				723.19	100.00

Table B. 3:Uplif capacities of pile with length 15m

T= 0 (Pure uplift load), d=0.6m		T= 0 (Pure uplift load), d=0.8m		T= 0 (Pure uplift load), d=1.0m	
Uplift laod(kn)	Vertical displacement(mm)	Uplift laod(kn)	Vertical displacement(mm)	Uplift laod(kn)	Vertical displacement(mm)
0.00	0.00	0.00	0.00	0.00	0.00
44.54	1.19	55.71	1.20	57.07	1.28
133.57	3.56	167.03	3.59	171.21	3.83
221.92	5.93	277.88	5.99	399.44	8.93
397.86	10.68	498.17	10.78	625.73	14.03
736.13	20.17	717.30	15.58	737.84	16.58
1020.46	29.67	934.76	20.37	960.81	21.68
1222.15	39.16	1146.88	25.16	1178.79	26.78
1239.93	43.91	1348.73	29.96	1384.42	31.89
1244.63	48.65	1536.31	34.75	1571.95	36.99
1242.37	53.40	1710.70	39.54	1745.11	42.10
1240.38	60.00	1868.96	44.33	1898.68	47.21
		2006.67	49.13	2028.81	52.33
		2119.18	53.92	2185.43	62.57
		2171.37	58.71	2184.80	72.83
		2184.81	63.51	2177.34	93.35
		2180.62	68.30	2174.98	100.00
		2172.36	77.88		
		2172.24	80.00		

Appendix C: Lateral response

C.1: Lateral Load Capacity

Table C. 1: The lateral capacities for lateral deflection of 0.1D lateral load of pile 5m length with different diameters.

T= 0 (Pure uplift load), d=0.6m		T= 0 (Pure uplift load), d=0.8m		T= 0 (Pure uplift load), d=1.0m	
Lateral laod(kn)	Horizontal displacement(mm)	Lateral laod(kn)	Horizontal displacement(mm)	Lateral laod(kn)	Horizontal displacement(mm)
0.00	0.00	0.00	0.00	0.00	0.00
4.86	0.68	6.55	0.80	7.65	0.84
13.89	2.03	18.86	2.41	22.55	2.53
22.24	3.38	30.22	4.01	36.06	4.22
30.06	4.72	40.81	5.62	61.44	7.59
44.91	7.42	60.88	8.82	73.25	9.27
51.86	8.77	79.66	12.02	96.03	12.64
65.32	11.46	96.88	15.22	116.70	16.00
77.53	14.15	112.84	18.41	153.74	22.72
88.84	16.84	127.51	21.61	170.19	26.08
99.35	19.53	141.18	24.81	185.45	29.44
108.94	22.23	153.81	28.01	199.89	32.79
117.90	24.92	165.40	31.20	226.47	39.51
126.37	27.61	176.16	34.40	238.35	42.87
134.42	30.30	186.33	37.60	260.03	49.59
142.01	33.00	195.95	40.80	279.60	56.30
148.97	35.69	205.02	43.99	297.57	63.02
155.58	38.38	213.53	47.19	314.43	69.74
161.80	41.08	221.66	50.39	330.09	76.46
167.73	43.77	229.37	53.58	344.96	83.18
178.76	49.16	243.86	59.98	359.09	89.90
188.97	54.54	256.99	66.38	379.27	99.98
198.47	59.93	269.10	72.77		
198.57	60.00	280.24	79.17		
		281.61	80.00		

Table C. 2: The lateral capacities for lateral deflection of 0.1D lateral load of pile 10m length with different diameters.

T= 0 (Pure uplift load), d=0.6m		T= 0 (Pure uplift load), d=0.8m		T= 0 (Pure uplift load), d=1.0m	
Lateral laod(kn)	Horizontal displacement(mm)	Lateral laod(kn)	Horizontal displacement(mm)	Lateral laod(kn)	Horizontal displacement(mm)
0.00	0.00	0.00	0.00	0.00	0.00
7.47	0.84	11.86	0.89	14.08	1.06
21.50	2.52	35.27	2.68	41.59	3.18
34.54	4.20	57.43	4.46	67.63	5.30
47.10	5.87	100.08	8.03	92.72	7.42
59.23	7.55	120.35	9.81	140.68	11.66
71.05	9.23	159.18	13.38	163.14	13.78
93.52	12.59	196.11	16.94	206.81	18.02
114.39	15.94	231.54	20.51	248.03	22.26
133.74	19.30	265.09	24.08	286.36	26.49
151.87	22.65	296.51	27.64	322.38	30.73
168.99	26.01	326.64	31.21	356.82	34.97
185.07	29.36	355.59	34.77	388.92	39.20
200.28	32.72	382.81	38.34	419.39	43.44
214.90	36.07	408.88	41.90	447.93	47.68
228.94	39.43	433.55	45.47	475.30	51.92
242.41	42.78	457.13	49.04	501.74	56.16
255.48	46.14	479.98	52.61	527.12	60.39
268.13	49.50	502.20	56.18	551.49	64.63
280.27	52.85	544.27	63.31	574.73	68.87
291.85	56.20	583.44	70.44	597.20	73.10
302.96	59.56	620.31	77.57	639.91	81.57
304.37	60.00	632.03	79.93	679.66	90.04
				716.86	98.50
				723.19	100.00

Table C. 3: The lateral capacities for lateral deflection of 0.1D lateral load of pile 15m length with different diameters.

T= 0 (Pure uplift load), d=0.6m		T= 0 (Pure uplift load), d=0.8m		T= 0 (Pure uplift load), d=1.0m	
Lateral laod(kn)	Horizontal displacement(mm)	Lateral laod(kn)	Horizontal displacement(mm)	Lateral laod(kn)	Horizontal displacement(mm)
0.00	0.00	0.00	0.00	0.00	0.00
8.02	0.90	12.37	0.81	16.92	1.12
23.06	2.69	36.71	2.44	50.00	3.34
37.00	4.49	60.15	4.06	81.62	5.57
50.45	6.28	82.99	5.68	142.25	10.03
63.41	8.08	105.31	7.31	199.23	14.49
76.06	9.87	127.17	8.93	253.83	18.95
88.27	11.67	148.60	10.55	305.46	23.40
99.94	13.46	190.35	13.80	354.51	27.86
122.20	17.05	230.65	17.05	400.91	32.31
142.91	20.64	269.16	20.29	445.34	36.77
162.19	24.23	306.10	23.54	487.16	41.23
171.27	26.02	341.55	26.78	527.05	45.69
188.97	29.61	375.78	30.02	565.39	50.15
205.76	33.20	408.73	33.27	602.31	54.61
221.69	36.79	440.41	36.51	638.51	59.06
236.94	40.38	471.00	39.76	673.36	63.52
251.74	43.97	500.66	43.00	707.04	67.98
265.98	47.56	529.20	46.25	771.63	76.90
279.58	51.15	556.87	49.49	832.57	85.83
292.68	54.73	583.75	52.74	889.71	94.75
305.35	58.32	635.38	59.23	921.45	100.00
311.06	60.00	684.21	65.72		
		730.91	72.21		
		775.84	78.70		
		784.61	80.00		